

EVALUATION OF THE THERMAL CHARACTERISTICS OF SOLID STATE  
RELAYS USED FOR HEAT TRACING APPLICATIONS

THESIS

Presented to the Graduate Council of  
Texas State University-San Marcos  
in Partial Fulfillment of the Requirements

for the Degree

Master of SCIENCE

by

Nicholas Miller, B.S.

San Marcos, Texas  
May 2009

EVALUATION OF THE THERMAL CHARACTERISTICS OF SOLID STATE  
RELAYS USED FOR HEAT TRACING APPLICATIONS

Committee Members Approved:

---

Carl A. Ventrice, Jr., Chair

---

Gregory F. Spencer

---

Nikoleta Theodoropoulou

Approved:

---

J. Michael Willoughby  
Dean of the Graduate College

**COPYRIGHT**

by

Nicholas Miller

2009

## **ACKNOWLEDGEMENTS**

I would like to thank Texas State University-San Marcos department of physics. The faculty of the physics department has always pushed me to educate myself as much as possible. At the time, I didn't understand why we (my fellow students and I) had to work so hard. In the past year I have developed my greatest appreciation for the physics department at Texas State. Four years ago I wasn't sure if I could graduate with a bachelor's degree (especially in physics). Two years ago I received my bachelor's in science but desired more education. The faculty believed I could continue my learning and receive a master's degree. As scared as I was, I enrolled and two years later turned in a thesis.

Next, I would like to offer a special thank you to my fellow students who have always supported me. Numerous occasions, they could sense the desperation and anxiety, but still helped me through the hard times. There is no doubt that I could not have been as successful in school without my Texas State physics classmates. They are a neat group of people who I am proud to call friends.

I also need to thank Doctor Carl Ventrice. Dr. Ventrice mentored me through, not just the graduate classes, but also my thesis. During graduate school, if there was ever a problem in any class, Dr. Ventrice had an answer. He also helped me develop my thesis through my work at Thermon, which is greatly appreciated.

Lastly, I would like to thank Thermon. Thermon allowed me to work and develop my thesis through the company. A special thanks to Roy Barth (V.P. of Research and Development), Ron Zaborowsky (Manager of Technical Services), and Mike Garcia (Product Specialist). These gentlemen supported my furthering of education from the first day I became employed at Thermon. They allowed me the time, materials necessary, and most of all helpful knowledge, while developing my thesis.

This manuscript was submitted on April 15, 2009.

## TABLE OF CONTENTS

	<b>Page</b>
ACKNOWLEDGEMENTS .....	iv
LIST OF FIGURES .....	vii
LIST OF TABLES .....	x
ABSTRACT.....	xi
CHAPTER	
1. INTRODUCTION .....	1
2. OVERVIEW OF RELAYS .....	3
2.1. Electromagnetic Relays Versus Solid State Relays.....	3
2.2. Theory of Solid State Relays .....	4
2.3. Applications of Solid State Relays for Heat Tracing .....	20
3. EXPERIMENT AND DESIGN .....	22
3.1. Background.....	22
3.2. Apparatus and Setup .....	23
4. TESTING AND DATA ANALYSIS .....	37
4.1. Targeted Powers .....	37
4.2. Installation of Fans and Vents .....	48
4.3. Results .....	50
5. DISCUSSION.....	53
6. CONCLUSION.....	54
REFERENCES .....	55

## LIST OF FIGURES

Figure	Page
2.2.1. Electromagnetic Relay .....	5
2.2.2. AC Solid State Relay .....	5
2.2.3. Top view of SSR.....	6
2.2.4. <i>PN</i> junction with depletion region (from reference 5).....	8
2.2.5. Biasing the <i>pn</i> junction diode (from reference 5) .....	10
2.2.6. Optically isolated DC input circuit .....	11
2.2.7. JFET .....	11
2.2.8. <i>N</i> -channel JFET .....	12
2.2.9. <i>N</i> -channel JFET after applying positive gate voltage .....	12
2.2.10. Ideal diode model for silicon .....	13
2.2.11. Diode symbol.....	13
2.2.12. Optically isolated AC output circuit .....	14
2.2.13. <i>Npn</i> epitaxial planar structure of the BJT .....	15
2.2.14. Biasing of <i>npn</i> BJT .....	15
2.2.15. BJT currents .....	16
2.2.16. Layered <i>pnpn</i> construction of thyristor.....	18
2.2.17. Thyristor circuit .....	18

2.2.18. Layered construction of SCR.....	18
2.2.19. Schematic symbol for SCR.....	18
2.2.20. Layered construction of triac .....	19
2.2.21. Schematic symbol for a triac .....	19
3.2.1. IP66 stainless steel free standing Saginaw panel.....	24
3.2.2. Instek Programmable Power Supply.....	24
3.2.3. Front view of variac .....	25
3.2.4. Top view of variac .....	25
3.2.5. Shunt resistor (0.01 Ohm) mounted to aluminum heat sink.....	26
3.2.6. Hydra series II.....	27
3.2.7. Cartridge inserted in back of Hydra.....	27
3.2.8. Inside of cartridge with thermocouples .....	27
3.2.9. Mounted heat sinks using Thermon’s custom made brackets .....	29
3.2.10. SSRs mounted to heat sink with SSR circuit board and ribbon cable .....	30
3.2.11. Crydom HD 6050 solid state relay .....	31
3.2.12. Finned heaters .....	32
3.2.13. Thermocouple locations on left side of panel (interior) .....	33
3.2.14. Overall schematic of test.....	36
3.2.15. Series circuit inside panel .....	36
4.1.1. Equilibrium conditions .....	39
4.1.2. Change in temperature versus power.....	40
4.1.3. Change in temperature versus power with linear similarities.....	41

4.1.4. Characteristic of SSR.....	44
4.1.5. Change in temperature versus power (two) .....	48
4.2.1. Top View of Panel .....	49
4.2.2. Right exterior view of panel .....	49
4.3.1. Change in temperature versus power (three) .....	50
4.3.2. Change in temperature versus power at five feet inside panel .....	51
4.3.3. Overall performance at five feet inside panel.....	52

## LIST OF TABLES

<b>Table</b>	<b>Page</b>
4.1.1. Downloaded hydra information .....	38
4.1.2. Similar voltages from graph .....	42

## **ABSTRACT**

### **EVALUATION OF THE THERMAL CHARACTERISTICS OF SOLID STATE RELAYS USED FOR HEAT TRACING APPLICATIONS**

by

Nicholas Miller, B.S.

Texas State University-San Marcos

April 2009

**SUPERVISING PROFESSOR: CARL VENTRICE JR.**

Unlike its predecessor, the electromagnetic relay, a solid state relay contains a switching capability with no moving parts. This process is accomplished through the utilization of solid state devices within the relay structure. Solid State relays can be photo-coupled, transformer-coupled, and hybrid [1]. This research project focuses on just the photo-coupled relays. The theory of the solid state relay (including how the relay works), a specially designed test involving these relays and the intriguing results of the test are discussed in detail in this thesis. The test that we designed, implemented, and discussed is pertains to the heat tracing industry. Heat tracing is the external application of heat to pipes, tanks, and instrumentation. Solid state relays are used as control switches which communicate with a heat tracer telling it when to turn on and off. The

power through the relays while in the “on” state will result in internal heat formation. Thermal properties of the solid state relay expose their limitations in the heat tracing field. Once these limitations are tested and analyzed, decisions can be made about the applications of solid state relays used for a particular heat tracing application.

# **CHAPTER 1**

## **INTRODUCTION**

Solid state relays are electronic switches used to control the “on” and “off” functions of an electrical circuit. They contain the same performance capabilities as an electromagnetic relay but without moving parts. The switching process of the solid state relay depends upon electrical, magnetic and optical properties of semiconductor devices [1]. When engineered correctly, the semiconductors separate the output from the input in a solid state relay switch until communicated otherwise.

Solid state relays are fast becoming the switches of choice in heat tracing. They control the power delivered to a heat tracing cable. Heat tracing, by definition is the external application of heat to pipes, tanks and instrumentation. The following research was performed at Thermon (a company that specializes in heat tracing). Thermon uses solid state relays in control panels for heat tracing cables which are distributed throughout different pipe orientations at chemical plants, petroleum plants, and offshore rigs etc. These relays are activated by specialized Thermon controllers which are mounted inside the same control panel as the solid state relays.

Solid state relays, when conducting (“on”), produce heat from internal power dissipation. This is a concern when using solid state relays. At manufacturer specified internal temperatures of the solid state relays, a form of break down will occur and the relay will malfunction and possibly self-destruct. Heat sinks are used to absorb and

redistribute the heat from the relays. The following paper will test these relays, along with their heat dissipation while installed in a closed environment.

The research begins with an overview of relays (more specifically the solid state relay). The overview includes a macro discussion of the physics involved in the building of semiconductor devices and then the engineering of these devices to perform specific duties of the solid state relay. The testing focuses on the thermal characteristics of solid state relays while in the conducting state with various power dissipations in a controlled environment. This testing is specific to Thermon's research and development department, but enables a greater understanding of the solid state relays performance while operating.

## **CHAPTER 2**

### **OVERVIEW OF RELAYS**

#### 2.1 Electromagnetic Relays Versus Solid State Relays

Solid state relays (SSR) are electronic switches which contain no moving parts. They depend solely on the electrical and optical properties of semiconductors used within the relay. This characteristic enables SSRs to have an advantage over their predecessor, the electro mechanical relay (EMR). SSRs have proven to be faster in response time due to the fact that the switching time is in direct relation with the amount of time needed to turn an LED (light emitting diode) on or off. In addition, since SSRs lack movable parts, they can be used in explosive environments such as chemical plants because no spark is generated while the SSR is switching. The SSRs also have longer lives than the EMRs because, once again, there are no moving parts to wear out and no arcing contacts to deteriorate. The SSRs are also noiseless (acoustically). Of course, with advantages there are also disadvantages when comparing the SSRs to the EMRs. Although acoustically SSRs are quiet, they create a lot of electrical noise while conducting. With SSRs there is a reverse leakage current that must be accounted for while the SSR is “off” (open). SSRs are also vulnerable to voltage transients which will cause unwanted switching. When comparing the two types of relays monetarily, the SSR is more costly as well [1,2]. The advantages of the SSRs when compared to the disadvantages are

weighed heavily in the heat tracing field. For example, if there is a concrete freeze protection package being sold to a new parking garage, and the control room is outside and not in a flammable environment, then an EMR is a good option. Let's now say that the parking garage is for a nuclear power plant and not only is the garage heat traced but so are the pipes in the plant. This is considered a hazardous location in which extreme measures are taken to ensure no sparks. Solid state relays meet this requirement

## 2.2 Theory of Solid State Relays

A relay is a switch that opens and closes by means of control from another electrical source. Another way of explaining this is through example. In order for a circuit to be complete, there must be an uninterrupted path from a negative to a positive source (not necessarily in that order) and some sort of resistive load for the current to flow through. If the path is broken then current will not exist and cannot pass through the relay to the load. A relay can open and close this loop so that when the relay is "on", the switch is closed and the current loop is energized. When the relay is "off", the switch is open and there is a break in the loop which will not allow current to flow. The relay switching is controlled by an alternate source of power. This control is attached to the input terminals of the relay while the output terminals consist of the load circuit leads.

In principle, solid state relays work like the electro mechanical relays. While the switch is open, the relay isolates the input from the output. Once the switch is closed, the necessary circuit loop is formed and energy can be transferred. What separates the two is how this process is accomplished. The EMR uses magnetic coupling while the SSR utilizes photo coupling. An electromagnetic relay configuration can be seen in Figure 2.2.1.

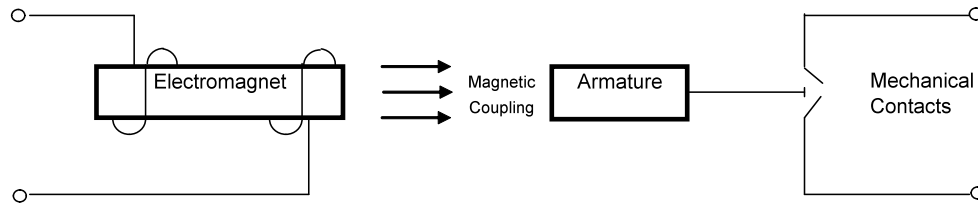


**Figure 2.2.1: Electromagnetic Relay**

The electromagnet is composed of an iron core containing many turns of fine magnetic wire. When this electromagnet is energized an attraction takes place between the pivoting armature and contacts. Once the contacts touch, a power circuit has been created [1,2].

Solid state relays in contrast, utilize photo coupling instead of magnet coupling as shown in Figure 2.2.2. Once a direct current voltage is applied on the input side of the SSR, a light emitting diode illuminates. This light arrives at the photo detector (photosensitive diode), which then electrically drives the triggering of the output device of the SSR. Output devices in an SSR can vary from one relay to another. The output device involved in the following paper is discussed in greater detail as the SSR circuitry is further analyzed. The RC snubber in Figure 2.2.2 restricts any swift voltage changes which can unintentionally turn the output device on.

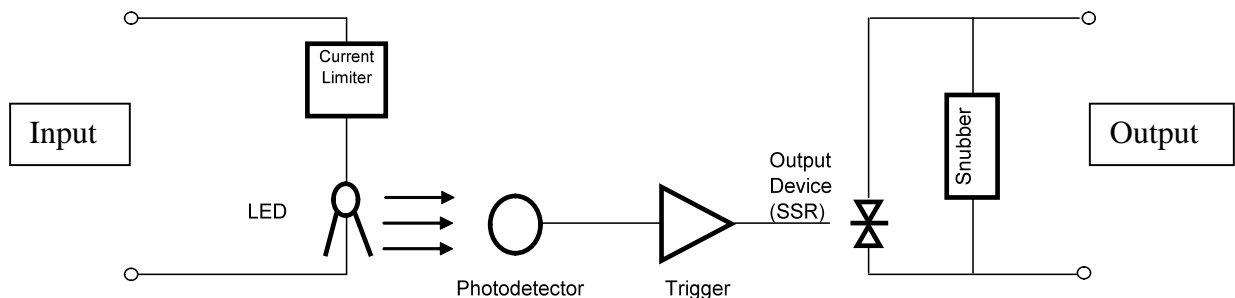


**Figure 2.2.2: AC Solid State Relay**

The relays used in this particular research are composed of a direct current (DC) control input and alternating current (AC) control output. The type of SSR is defined by the output current, so in this case an AC SSR would be the proper title. The SSR is best explained by first looking to the input design or the left side of Figure 2.2.2 [1,2].



**Figure 2.2.3: Top view of SSR**

The DC input supplies the relay with a control voltage. The SSR receives the control voltage through its input terminals which are located on one side of the relay (Figure 2.2.3).

Before the detailed discussion on how solid state relays work, an overview of the p-n junction in semiconductors is helpful. By definition a semiconductor is a material that acts as an insulator at low temperatures and a conductor at elevated temperatures due to their small band gap. Silicon has a band gap of 1.1eV and is the most common of semiconductors, especially in the solid state relay. The conductivity of semiconductors is increased by alloying the semiconductor with small amounts of impurity atoms, which is called doping. Doping effectively adds electrons or holes to a semiconductor material. The SSR is composed of mostly semiconducting electronic devices. These electronic devices utilize *p-n* junctions in order to operate. The *p-n* junction is essential when trying to rectify, amplify, and more importantly to this research, a current “off” and “on” switch, in electrical circuits. Consequently, to have a *p-n* junction, there must be a *p*-type and an *n*-type semiconductor in contact with one another. *N*-type semiconductor refers to

electron doped semiconductor which brings the Fermi level towards the conduction band. *P*-type semiconductors in contrast contain extra holes which forces the Fermi level towards the valence band [3,4,and 5]. Pictures of the band gap in the doped materials, as well as the Fermi levels, are shown in Figure 2.2.4. Once two pieces of silicon doped with a *p*- and *n*-type come into contact with each other there is a *pn* junction formed at their boundary. Electrons and holes, like most particles, have a natural desire to go from a highly concentrated area into a lower concentrated area. Because of this effect, the electrons and holes closest to the junction diffuse into the opposite side leaving uncompensated positive and negative ionized dopant atoms in their once occupied space. This process is called carrier diffusion. The two layers of negative and positive charges form a dipole depletion or transition region with an equal positive space charge region near the *n*-side as the negative space charge region near the *p*-side. This dipole will create an electric field from positive to negative charges (refer to Figure 2.2.4). Also in Figure 2.2.4 is the electrostatic potential  $V_0$ . This is the potential voltage formed across the two different gradients of the *n*-type and *p*-type silicone. The potential barrier restricting current flow across the space charge region is equal to the contact potential multiplied by the elemental charge ( $q$ ).

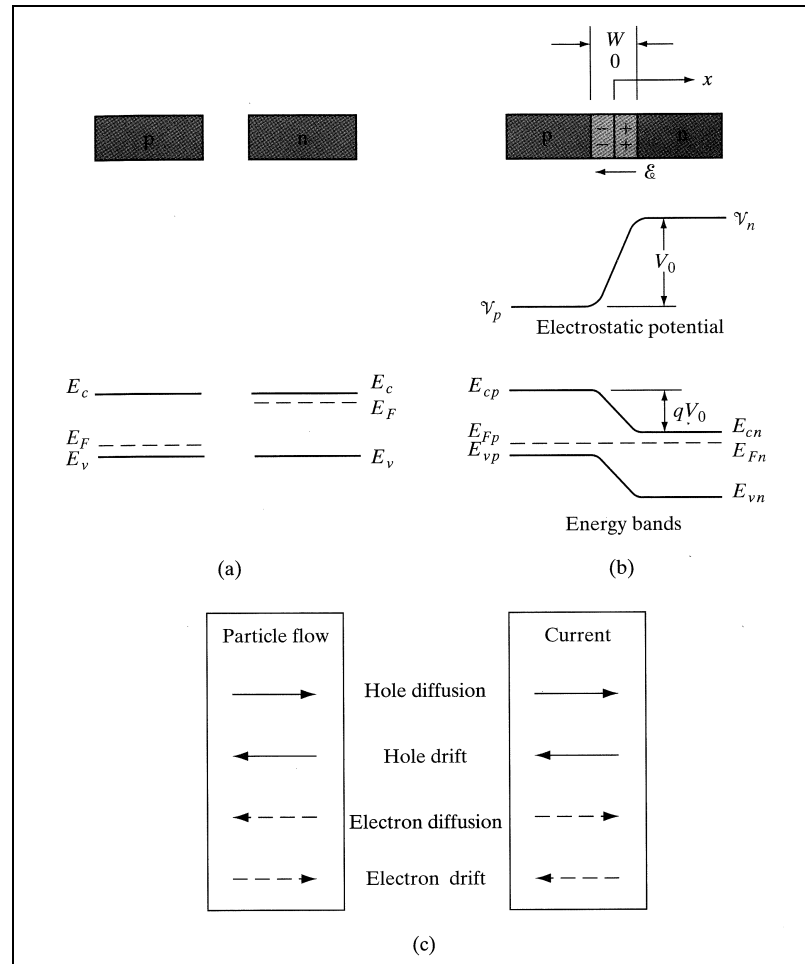


**Figure 2.2.4: PN junction with depletion region (from reference 5)**

The band bending in Figure 2.2.4 after contact is made between the two materials is a result of the Fermi level alignment of the materials. Looking to the band bending in the above figure, there is now a “potential hill” that an electron must climb in order to reach the conduction band in the p-type material. Lastly, look to the magnitude and direction of the electron and hole drifts in the above figure. In this particular state the  $p$ - $n$  junction has a net flow of current equal to zero. Since there is a diffusion current traveling from  $p$ -type material to  $n$ -type material, then there must be a current equal in magnitude but opposite in direction. This current is produced by electron-hole pairs being swept out of the space charge region and is known as drift current [5].

A bias voltage can now be applied to the  $p$ - $n$  junction resulting in a diode response. Forward biasing decreases the potential barrier allowing diffusion current to increase [5]. By connecting the  $n$  region to the negative terminal and the  $p$  region to the positive terminal of a voltage source, the forward biasing condition has been met. Now that the negative terminal of the battery is connected to the  $n$ -type material and like charges repel, the electrons in the  $n$ -type material will want to proceed as far from this incoming negative voltage as possible. This flow of electrons is known as electron current. Now, there exists an applied electric field which is opposing the previously discussed built in electric field which causes an over-all decrease in the electric field within the transition region. The result of the changing electric field and the increasing number of electrons and holes flowing into the depletion region, have an effect on the depletion width. The electrons decrease the amount of positive charges while the holes decrease the amount of negative charges that made up the depletion region [3,4]. The resulting decrease in the depletion region can be seen in the following figure. Notice the smaller depletion region and potential barrier after forward biasing in Figure 2.2.5.

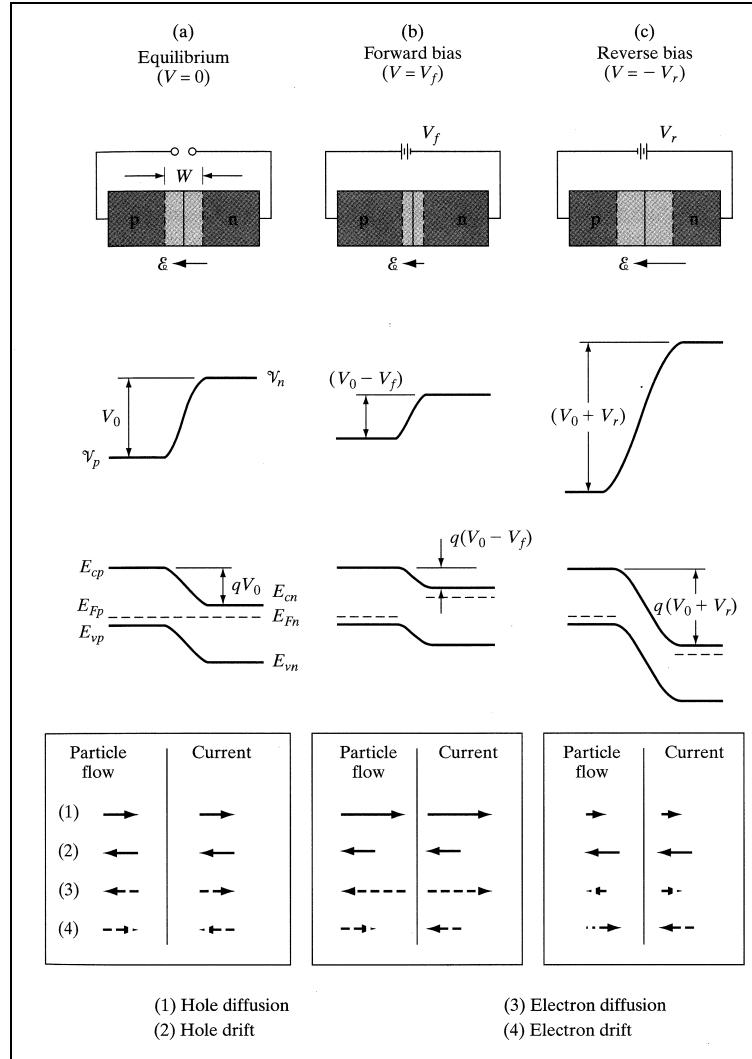


**Figure 2.2.5: Biasing the *pn* junction diode (from reference 5)**

The forward biasing procedure exponentially increases the probability that charge carrier will diffuse across the transition region so that the current passing through a forward biased diode increases exponentially. This is mathematically explained using equation 1.

$$I = I_0(e^{\frac{qV}{kT}} - 1) \tag{1}$$

Notice the exponential increasing current as the forward bias voltage is increased. When the *p-n* junction is reverse biased by switching the polarity of the voltage leads, then the exact opposite would happen with an increase in the size of the depletion region,

increasing the size of the potential barrier and essentially restricting the current flow (Figure 2.2.5). The result of this biasing using equation 1 is the exponential term going away, leaving a small reverse bias current. The drift current throughout the biasing process is unaltered due to the fact that electron hole pairs being swept out of the depletion region is based on how often this process takes place and not how quickly. This basic knowledge of the  $pn$  junction is important in understanding the semiconductor devices involved in the SSR [5].

Just the input control circuit with the current limiter and light emitting diode in the SSR are shown in Figure 2.2.6.

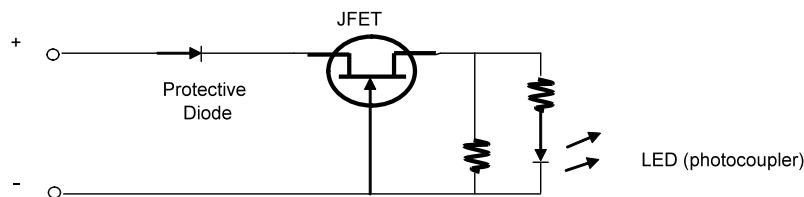


**Figure 2.2.6: Optically isolated DC input circuit**

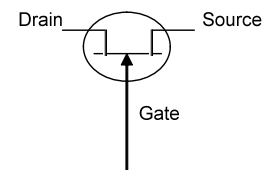


**Figure 2.2.7: JFET**

Current is limited by the n-channel junction field-effect transistor (Figure 2.2.7). In general, a transistor is a three terminal device often used in electronics as an amplifier for small a-c signals or as an on/off switch. A field effect transistor (FET) is unipolar, unlike the bipolar junction transistor (BJT). This means that BJTs use both electron and hole current, while FETs utilize just one type of charge carrier (majority carrier). Charge carriers can be either electrons or holes. In addition, unlike the BJT, the amount of voltage controls the current through the FET, while the BJT is current controlled. The junction field-effect transistor (JFET) is a special type of field effect transistor. The control (gate) voltage of the JFET works by varying the depletion width ( $W$ ) of a reverse-

biased hole-electron (p-n) junction. By varying  $W$ , current between the drain and source can be manipulated [1,2].

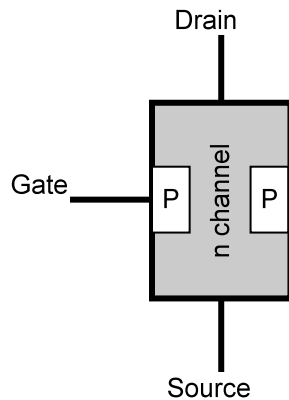


**Figure 2.2.8: N-channel JFET**

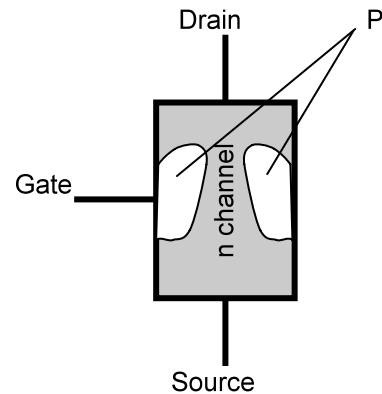


**Figure 2.2.9: N-channel JFET after applying positive gate voltage**

The growth in the width of a  $p$ - $n$  junction is shown in Figure 2.2.8 and Figure 2.2.9, which restricts the amount of current flow between the drain and source. Keep in mind, the gate leads are connected to both p-type regions. The gate to source voltage that is reverse biased controls the way the JFET operates. The negative gate voltage being applied to the p-doped region causes a depletion region between the p-n junctions. By increasing the gate to source voltage, the depletion region is increased and continues to narrow the n-channel. The narrower the channel width the less drain current is produced due to the increased resistance in the now narrowing travel space (Figure 2.2.9). The result of this process is a current limiter. Current is limited in order to protect the light emitting diode from extreme current conditions [1,2].

The physical understanding of the light emitting diode as well as the protective diode can be continued from the formerly mentioned  $pn$  junction. The diode is a device containing a p-n junction that when forward biased allows current to pass through this junction. The potential required to cause a large increase in current is around 0.7 volts.

If reverse biased the diode acts as an open switch. The electrons and holes are pulled away from the junction. This dramatically increases the potential barrier that is necessary for the electrons to cross. Figure 2.2.10 below shows the characteristic curve of an ideal diode [3].

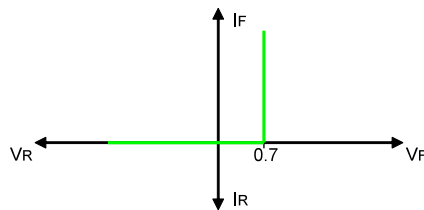


**Figure 2.2.10: Ideal diode model for silicon**



**Figure 2.2.11: Diode symbol**

Keep in mind the figure above is an ideal diode model in a non ideal world. In reality there is a small reverse current as well as an exponential increase in the forward current (equation 1). An LED is a type of diode that when forward biased releases energy from the recombination process (combining of electron-hole pairs). The free electrons are initially in higher energy states in the conduction band. As a result of the recombination process both heat and light energy result, as a form of conservation of energy. In this particular circuit (Figure 2.2.6); the LED uses this energy to bridge the input and output in the form of photo coupling (detailed further down). The light energy shown by the LED is converted electrical energy initiated by a controller. The protective diode in Figure 2.2.6 is used as a safety precaution. The diode opposes unintentional reversal of voltage which could destroy both the JFET and LED. If the voltage reverses, the diode becomes reverse biased and in this case an open switch as discussed before [3].

Photo coupling is the name given to the process that the SSR uses to communicate the input to the output without moving parts (like in the EMR). This document continues now with a detailed discussion on how this transition is made from input to output or left

to right when looking at Figure 2.2.2, along with the electronic devices and switches involved in the output of the relay. The LED on the input side is able to communicate with the phototransistor (photo-silicon controlled rectifiers). This is done through the infrared light energy the LED produces, in which the phototransistor receives. The phototransistor receives light energy and converts it back to electrical energy, which entail bridges the input and output. Further detail of this process as well as the output circuitry is discussed in the following paragraphs.

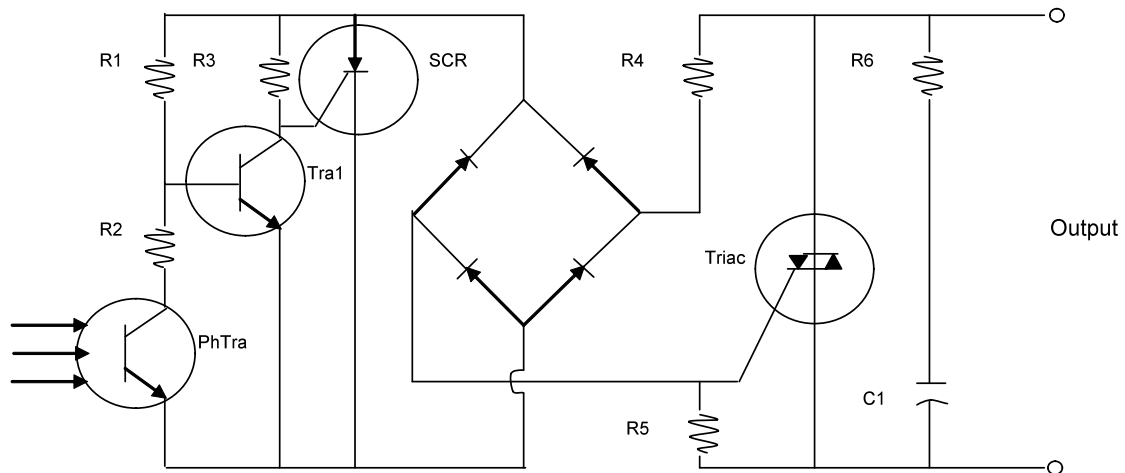


**Figure 2.2.12: Optically isolated AC output circuit**

The output schematic of an optically coupled AC SSR circuit is shown in Figure 2.2.12. The phototransistor (PhTra) on the far left works basically the same as a bipolar transistor that is briefly mentioned. The main difference is that light is used to create electron-hole pairs instead of a voltage source. This is better explained by first detailing the BJT. The structure of an *npn* bipolar junction transistor is shown in Figure 2.2.13. BJTs are used as current amplifiers in circuits [1,2].

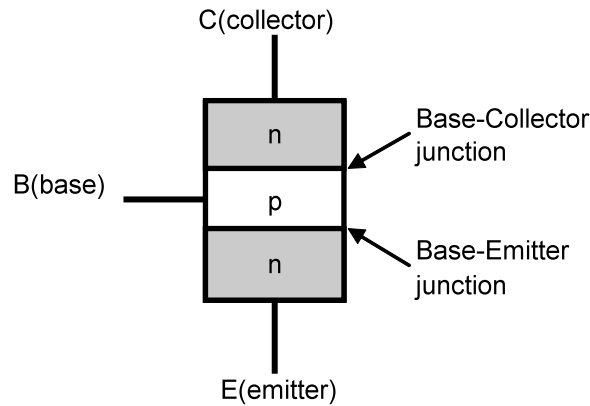


**Figure 2.2.13: *Npn* epitaxial planar structure of the BJT**

In order for the transistor above to be operational, the base-emitter (BE) junction is forward biased while the base-collector is reverse biased (Figure 2.2.13). The biasing creates a narrow depletion region at the BE junction and a large depletion region at the BC junction.

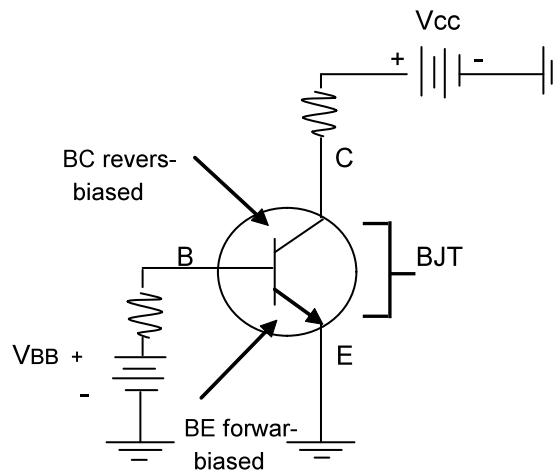


**Figure 2.2.14: Biasing of a *npn* BJT**

The emitter is heavily doped with electrons which are now teaming up with conduction-band free electrons that are diffusing through the BE junction into the *p*-type base region where they become minority carriers. The base, unlike the emitter is slightly doped with holes. This characteristic causes only a few of the now abundant electrons to pair with

the holes. The few that do recombine will cause a small base current as they flow out of the base lead as valence electrons. The rest of the electrons produce a large amount of electron flow into the base-collector (BC) depletion area. The electrons are then pulled through the reverse-biased BC region via the electric field that has been created by the attractive force between the positive and negative ions. The now large flow of electrons can continue on through the collector lead and out of the transistor. Note that the base current is much smaller than the collector current and therefore establishing the current gain or amplification of the BJT. The currents involved in the *npn* BJT along with their direction of flow are shown in Figure 2.2.15.

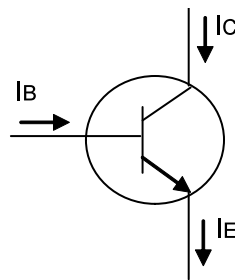


**Figure 2.2.15: BJT currents**

The collector current is represented by  $I_C$ ,  $I_B$  represents current through the base, and  $I_E$  is the symbol for the emitter current. Once again the phototransistor operates the same way as the BJT except that the base current is produced by light and not a voltage source [3].

Recalling Figure 2.2.12 the second transistor to be discussed is the BJT labeled Tra1. The phototransistor controls the Tra1 switching, while the Tra1 switching controls the triggering part of the SSR (refer to Figure 2.2.12). Tra1 is also designed to implement the zero turn-on features in the SSR. The zero turn-on features are first established by the control side or input of the SSR, being turned off. With the LED not illuminated the phototransistor is in a cutoff or “off” state. The phototransistor in this

state can be treated as an open circuit [1,2]. Tra1 is in an allowed saturation state (“on” state). Saturation means that the base and collector current are positive and sufficiently large. During saturation a large amount of current flows through the collector with a small voltage drop across the collector and emitter. With Tra1 saturating the silicon controlled rectifier can not come on which means the triac is off and the SSR is off. Once voltage on the input side is enough to light the LED, the phototransistor turns on. The two resistors R1 and R2 act as a voltage divider and have values so that Tra1 will remain on if the instantaneous line voltage is above zero. This keeps the SSR in an off position. When the line voltage approaches zero with either a positive or negative value, the phototransistor holds Tra1 out of saturation so that the SCR will trigger. Both of these devices are examined in greater detail in the following paragraph. The phototransistor does this by changing the bias of the Tra1’s emitter essentially making Tra1 a short circuit. The silicon controlled rectifier (SCR) next signals the triac to turn on completing the output circuit and therefore turning on the SSR. The four diodes in Figure 2.2.12 that are connected in what looks like a rotated square, is a bridge full-wave rectifier. The bridge rectifier ensures the SCR to trigger the triac for both the positive and negative cycle of the source. Detailed descriptions of the SCR and the triac are in the following paragraphs [1,2].

Both the SCR and the triac are AC switches commonly known as thyristors. Thyristors are four layered devices consisting of two *p*-type and two *n*-type semiconductor layers in alternating sequence. These devices can be described as two transistors in the same circuit which can be viewed in Figure 2.2.16 and Figure 2.2.17. One of the transistors is a *pnp* and the other is an *npn* transistor [3].

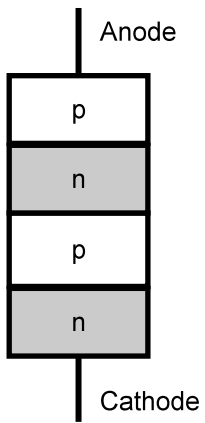


**Figure 2.2.16: Layered *pnpn* construction of thyristor**

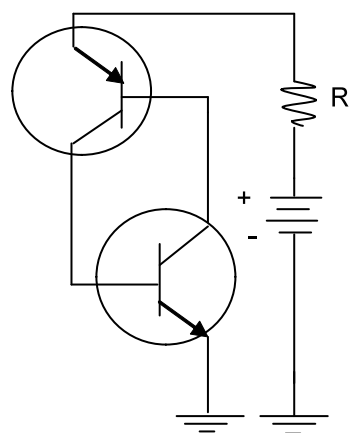


**Figure 2.2.17: Thyristor circuit**

The SCR is a specific four layer thyristor containing three terminals (Figure 2.2.16). In the “off” state the SCR can be thought of as a resistor with a really high resistance. In the “on” state the SCR is simply a short with a really low resistance.

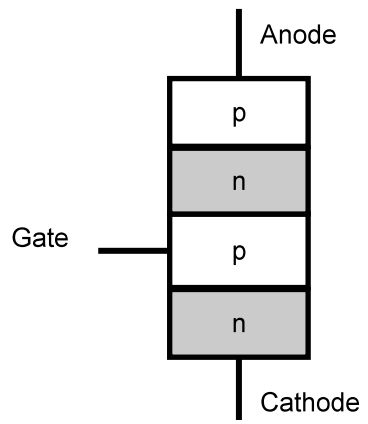


**Figure 2.2.18: Layered construction of SCR**

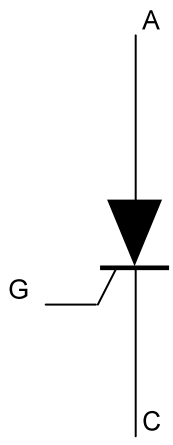


**Figure 2.2.19: Schematic symbol for SCR**

Once the SCR is triggered by a positive pulse (in this case the line voltage), both internal transistors will turn on (refer to Figure 2.2.17). Once the SCR is triggered and the phototransistor is no longer holding  $T_{ra1}$  out of saturation (triggering pulse over), the SCR will still remain on. The SCR will stay on even when the gate is receiving zero volts because of the two different transistors together. The transistors will supply each

other the necessary current (holding current) in a cyclical fashion. In order to turn the SCR off, the anode current must decrease below the holding current. This is done by decreasing the load current below the holding current. The triac used in the SSR circuitry is like the SCR, but is able to conduct current in both directions so that the polarity of the voltage across a triac will not matter. The triac, like the SCR, contains three terminals. The triac is basically two SCRs in parallel to each other containing a common gate terminal as seen in Figure 2.2.20 [3].

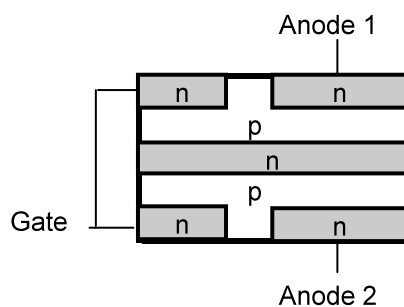


**Figure 2.2.20: Layered construction of triac**

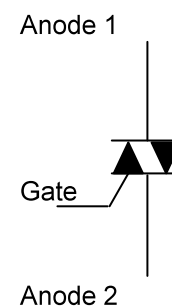


**Figure 2.2.21: Schematic symbol for a triac**

This arrangement allows triacs to conduct current in both directions. This bilateral current carrying mechanism is perfect when distributing current to a load using ac current. Triacs can easily be turned on by a small pulse or gate current (in this case the SCR provides the pulse). The triac used in the SSR configuration will remain on by being triggered every half cycle by the SCR. In order to turn the triac off, the anode current must drop below the holding current like the SCR. This can be accomplished by removing the input control and the AC line current drops to zero [1,2].

All of these switches being off constitute zero power to the load. There is however one problem using thyristors in the circuit. They are susceptible to rate effect which causes inadvertent turn-on without an actual gate signal. This problem is fixed

with the previously designed RC snubber. The snubber consists of capacitor C1 and resistor R6 found in Figure 2.2.12. The capacitor and resistor in series reduces the change in voltage with respect to time between the output terminals [1,2].

To summarize, once a large enough input voltage is applied to the LED so that the light turns on, the phototransistor will also turn on. The phototransistor will then hold Tra1 out of saturation in order to trigger the SCR which will turn on the triac. Turning on the triac completes the current loop allowing the output terminals to deliver power to the load. The SSR remains on until either the dc control is turned off or the ac output is dropped below a threshold voltage.

### 2.3 Application of Solid State Relays for Heat Tracing

The goal of this research project is to examine the thermal characteristics of solid state relays when used as control switches applicable to heat tracing. By definition, heat tracing is the external application of heat to pipes, tanks, and instrumentation. For instance, a petrochemical plant often requires that the chemicals in the pipes be kept at a constant temperature. The heat tracers used in this process are controlled (switched on and off) by solid state relays. This research is designed to better understand the physical parameters of the solid state relay that govern its performance under various power and temperature conditions.

While the SSR is conducting, there is a tremendous amount of heat produced. Attaching the SSRs to heat sinks greatly dissipates this heat off the electronics so they may work more efficiently and not malfunction due to overheating. Heat sinks utilize thermal contact to transfer heat. This particular research involves heat sinks that are nineteen by ten and one-half inch anodized extruded aluminum. Each heat sink is then mounted to

the outside of a control panel so that the heat is transmitted from relay to the outside of the panel. Keep in mind the solid state relays themselves are still inside the panel.

## **CHAPTER 3**

### **EXPERIMENT AND DESIGN**

#### 3.1 Background

In Europe there is a desire to have control panels occupy as little space as possible. The control rooms in Europe are small and the easiest way to minimize the amount of room control panels occupy, without changing actual panel design is to mount heat sinks inside the panel. Originally heat sinks are mounted to the outside of the panel which increases the physical width of the panel by three inches. In addition there needs to be room between panels so that the heat sinks may breathe. With the sinks mounted inside, the panels can be positioned right next to one another. Of course there must be a way to dissipate heat out of the panel without the use of external heat sinks. This can be done with the use of vents and/or fans.

Tests are designed in order to develop a rise in temperature as a function of power through a control panel. The maximum temperature must stay below the manufactured maximum solid state relay temperature operating range (125 °C). These tests are first conducted with a panel completely closed in. Once this testing is complete, holes will be cut into the panel so that fans and vents may be mounted. The tests are then repeated so that the effects of the fans and vents can be analyzed. The heat inside the panel is produced by the solid state relays. The following tests are conducted at different power levels, as well as varying the amount of air circulation through the panel.

If the relay is operating as an ohmic device, the experimentation should result in a linear temperature versus power graph due to the power to heat relation. In theory, when power is delivered through a SSR there is a heat loss. This heat loss should be linear when plotted as a function of power delivered to the complete circuit if the relay is operating as an ohmic device. In other words, the more power an SSR receives the more heat it dissipates. These results will then be used to evaluate which of the following scenarios (including the installation of fans and vents) is compatible for the European heat tracing market. Results need to include a plot of the change in temperature (inside panel temperature minus outside ambient temperature) versus power inside panel. The targeted powers are one hundred watts, two hundred fifty watts, five hundred watts, and seven hundred fifty watts. Each test is conducted until the change in temperature is at a relative steady state.

### 3.2 Apparatus and Setup

The IP66 stainless steel free standing Saginaw panel being used is two feet deep by three feet wide by five feet tall (Figure 3.2.1). The steel panel is painted and contains a full back plate, half swing out panel on front, viewing window, and sides are sealed with cover plates installed over pre-existing heat sink holes.



**Figure 3.2.1: IP66 stainless steel free standing Saginaw panel**

The input control voltage for the solid state relays is supplied by the GW PSP-405 Instek Programmable Power Supply (Figure 3.2.2).



**Figure 3.2.2: Instek Programmable Power Supply**

This particular power supply is used to apply a direct current with a specific to experimentation voltage, current, and power.

Power stat variable auto transformers (variac), which are mounted to a rolling cart, supply the output load voltage (Figure 3.2.3 and Figure 3.2.4). One variac provides a variable output from 0 volts AC to 160% above the rated input supply. In other words, the variac could supply up to 190 volts AC output for a 120 volt AC input. The other variac provides a variable output from 0 volts to 120% above its rated input supply. This particular variance could supply 290 volts AC output for a 240 volt AC input. In this research a 120 and 240 volt alternating current wall outlet supplies these transformers with the necessary voltage. The variac can only withstand a maximum current of 18 amperes.



**Figure 3.2.3: Front view of variac**



**Figure 3.2.4: Top view of variac**

The cart, on which the variac is mounted, is customized with terminal blocks, toggle switches, a shunt resistor (Figure 3.2.5) and banana jacks so that users can easily record voltages and currents for the items being tested.



**Figure 3.2.5: Shunt resistor (0.01 Ohm)  
mounted to aluminum heat sink**

A shunt resistor enables current to be measured by taking a recorded voltage drop over a known, low resistance, resistor, and using Ohm's law to solve for current. This process is discussed in greater detail during the testing process. The 100 watt shunt (TGHGCR0100FE) resistor is mounted to an aluminum heat sink (more on heat sinks further down) which is mounted to the cart. Because this is a resistor, there will be heat generated that will need to be dissipated by the heat sink.

Temperature, voltage and current are recorded using a Fluke Hydra Series II (Figure 3.2.6) data acquisition unit. The Hydra enables these parameters to be recorded at specified time intervals. Once data have been collected, the information can be uploaded to a computer using the RS-232C interface that comes with the Hydra. Once the Hydra is connected to a computer, via the RS43 cable, the Fluke Hydra Logger is opened (which must be downloaded to the computer). The next step is going into setup mode, clicking on utilities, and then "upload scans". Be sure that the Hydra is turned on. The computer will now store the recorded data in an excel spreadsheet. Each Hydra contains twenty different channels. Each channel can record voltage (AC and DC),

resistance, frequency, and temperature. Channel one has a 300 volt maximum capability, while the rest of the channels offer a 150 volt maximum.



**Figure 3.2.6: Hydra Series II**

The Hydra comes with a Fluke Universal Input Module (cartridge) which is inserted in the back side of the instrument (Figure 3.2.7). This cartridge contains the terminals that correspond to each channel in the Hydra (Figure 3.2.8).



**Figure 3.2.7: Cartridge inserted in back of Hydra**

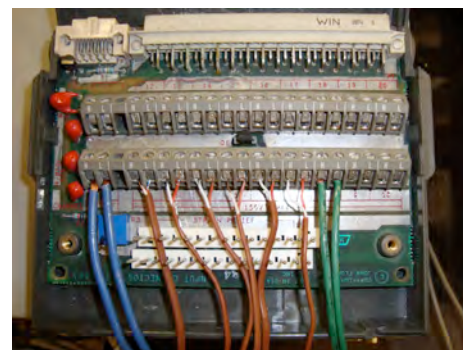


**Figure 3.2.8: Inside of cartridge with thermocouples**

Each channel has a high and low terminal which can receive either thermocouple wires or conductor wires. Thermocouples are used as temperature sensors in the following tests. They are based upon the principle known as the thermoelectric effect or Seebeck effect. This states that when a conducting metal receives a temperature change a voltage is

generated in the metal. When another conductor is connected to this active end, the second conductor will also experience an adjustment in voltage. The second conductor generates an opposing but equal in magnitude initial voltage (voltage drop). This voltage difference between the two enables the development of a temperature to voltage relationship. In the following test, the metal ends of the thermocouple are spot welded to make certain a good contact has been made. At this welded junction a change in temperature will cause a change in the voltage drop between the two metals. Each voltage drop has a corresponding temperature. The thermocouples used in these tests are a type J thermocouple which consists of iron and constantan. The temperature ranges for this thermocouple are from  $-40^{\circ}\text{F}$  to  $1,382^{\circ}\text{F}$ .

Inside the panel, four, aluminum, 19 inch by 10.5 inch, anodized extruded aluminum heat sinks, are installed three inches apart left to right and top to bottom, on a 10 gauge, 33 inch wide by 57 inch high, steel back plate (Figure 3.2.9). Thermon's heat sinks are used to dissipate heat from solid state relays. Six SSRs can be attached to one aluminum heat sink (SSR bank). Between the heat sink and each relay is a heat transfer compound to ensure good contact. Heat sink installation brackets were custom made by Thermon for easy installation.

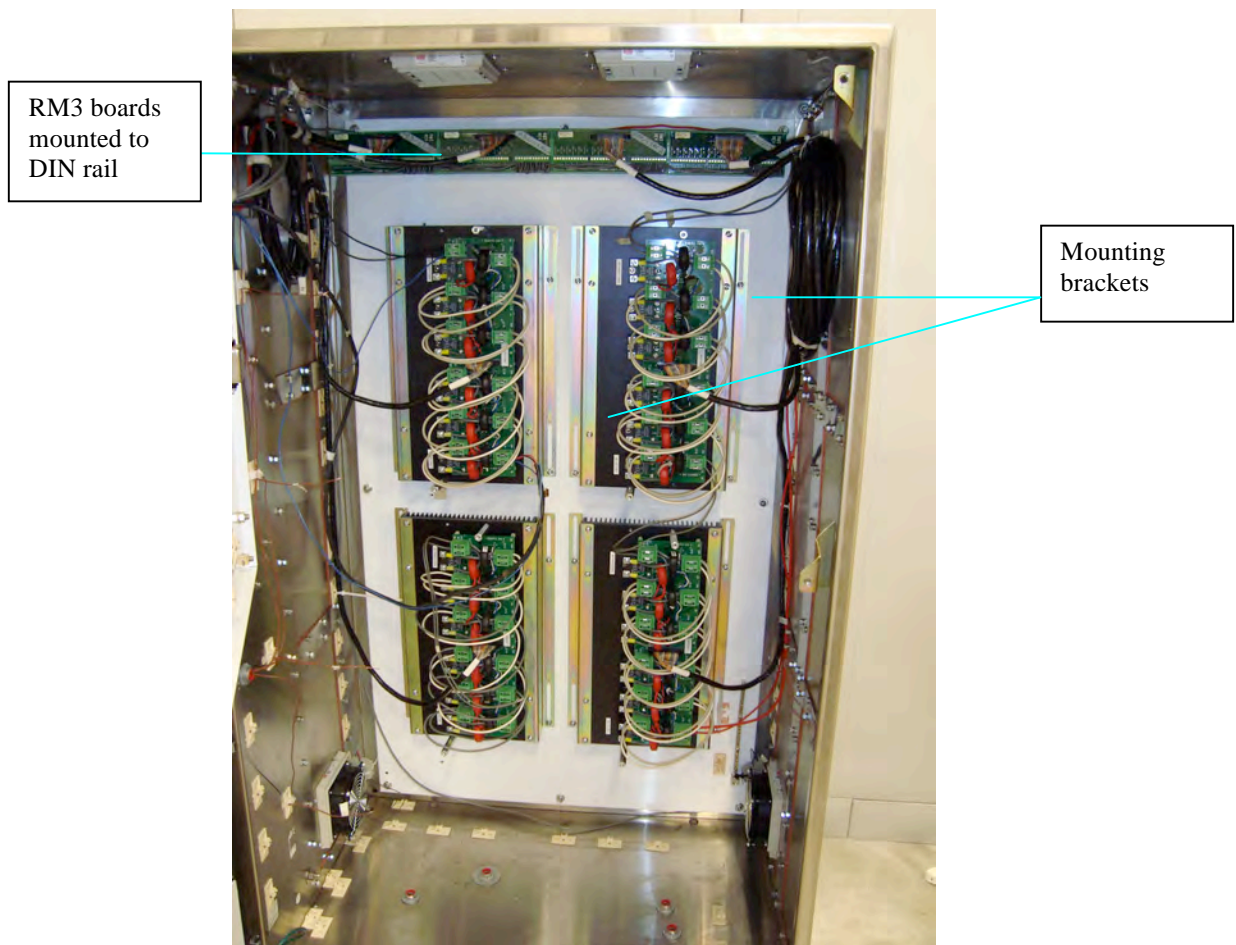


**Figure 3.2.9: Mounted heat sinks using Thermon’s custom made brackets**

The SSRs fasten directly to the heat sink using two placement screws. Mounted to the top of six SSRs is a circuit board so that the control voltage can be communicated to each relay (Figure 3.2.10). In the picture below there are also jumper wires connecting each SSR in series. The red and black objects are Thermon’s current detectors specially designed for the Thermon heat tracing controllers. They will not be a factor in this particular research. Din rail is mounted above the heat sinks on the same back plate (Figure 3.2.9). Din rail enables the placement of four RM3 circuit boards side by side (Figure 3.2.9). Each RM3 board contains six positive and six negative terminals. These

four RM3 boards offer communication from the control voltage to the SSRs (one RM3 board per SSR bank).

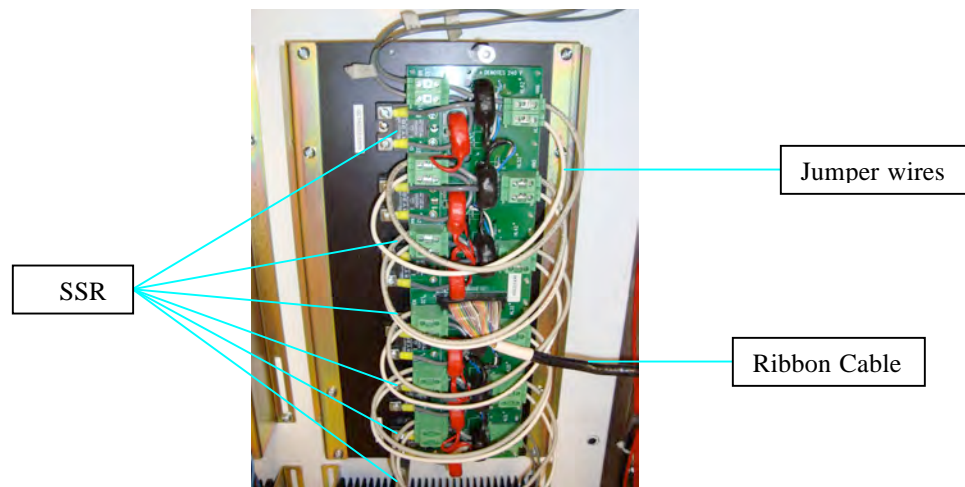


**Figure 3.2.10: SSRs mounted to heat sink with SSR circuit board and ribbon cable**

Fourteen gauge insulated conductor wires carry the energy from the power supply to the RM3 boards. Each positive and negative terminal on the boards, are connected in parallel via the same fourteen gauge wire used as jumpers. Ribbon cable is then used to carry the supply voltage from the RM3 boards to the SSR boards (Figures 3.2.9 and 3.2.10).

The load voltage being supplied by the variac is carried to the SSR output terminal blocks, by two twelve gauge insulated conductors. Each SSR has four corresponding terminal blocks for the load voltage leads. One pair of terminal blocks are used for an easy connection to the SSR output terminals while the other blocks make for an easy series connection between relays.

The solid state relay specific to this research is the Crydom HD 6050 (Figure 3.2.11).



**Figure 3.2.11: Crydom  
HD 6050 solid state relay**

There are four screw terminals located on top of the relay. The two smaller terminals are designated for the input voltage while the larger terminals are for the output voltages. The load voltage (output) range is from 48 to 660 volts (rms). The load current (input) ranges from 0.04 to 50 amps (rms). This SSR also has a maximum (peak) voltage drop of 1.7 volts during full rate load current along with a nominal 1.2 voltage drop while fully conducting. The input for the HD 6050 is controlled by a direct current source. Opposite to the two output screw terminals on the relay, there are two smaller screw terminals for the input. The control voltage range starts at three volts and ends at 32 volts (DC), with a typical input current of two mille amps (DC). This SSR operates with the maximum temperature of 125 °C (250 °F).

The resistive load found in Figure 3.2.12, pulls the current through the SSRs. They are finned strip heaters (3575K48) rated at 1900 watts when applying 120 volts (AC). Each heater has a resistance of  $8.8 \pm 0.3$  ohms. The heaters have been mounted to a fabricated frame with casters for easy mobility.



**Figure 3.2.12: Finned heaters**

These heaters are connected to the output terminal blocks of the SSR using twelve gauge insulated conductor wires. Once a voltage is applied to the heaters the resistance will begin to change because with an increase in heat, there is an increase in resistance. The amount of heating can be controlled slightly with a Dayton floor fan (MOD: 2LY93). The fan offers a constant cooling factor which allows more control over the test being run at a given time. Some of the following tests require the application of more than 140 volts to a heater. The fans oppose over heating of the loads as well as keep the current at a targeted value.

J-type thermocouples are installed at five different heights inside the panel starting at one foot and continuing to the top of the panel in one foot intervals (Figure 3.2.13). They are located on the left side of the panel with the welded junction positioned one foot off the side. They are then bundled together and ran out of the panel.

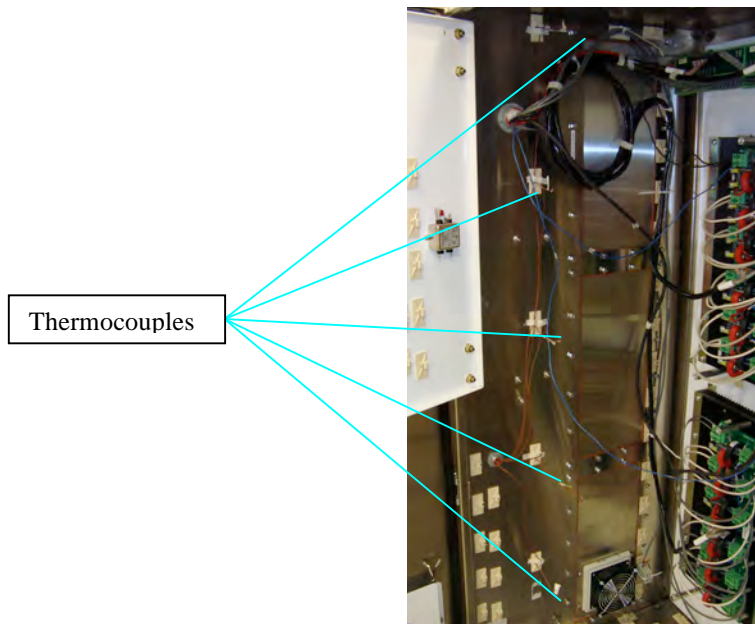


**Figure 3.2.13: Thermocouple locations on left side of panel (interior)**

There is also one thermocouple set outside the panel in order to record an ambient temperature. Each thermocouple will have a high (Iron) and low (Constantan) terminal in the Hydra's cartridge. Opposite to the Hydra the thermocouples are spot welded to ensure a good fusion of the two metals.

The Hydra is set to record voltage drops and six different temperature readings. The voltage drop across the relays can be recorded on the Hydra's first channel by placing two twelve gauge insulated conductor leads in one of the high and low terminals in the corresponding cartridge channel. Next, two wires of the same gauge as channel one, are placed in the second channels high and low terminals of the cartridge. These leads will record the voltage drop across the shunt resistor. All five thermocouples are now positioned into the same cartridge but separate channels. Each J-type thermocouple has a corresponding red and white lead. Proper installation of these thermocouples requires the red lead be place in the low (L) terminal while the white lead is placed in the

high (H) terminal. The thermocouple whose junction is located one foot high inside the panel is placed in the third position in the cartridge. The fourth position in the cartridge is for the thermocouple located two feet inside the panel. This numerical process is continued until all panel thermocouples are placed in the cartridge. The eighth cartridge terminal is for the ambient thermocouple. Once all thermocouples and voltage leads are installed the cartridge is ready to be placed in Hydra. The Hydra can now be turned on and programmed to the desired settings. Each channel can be reached by simply using the up and down arrow keys located on the front of the Hydra (Figure 3.2.6). By pressing the function key, then using the up and down arrows, the proper voltage (AC) selection can be established for channel one and two. Pressing the enter button will store the function and return the Hydra to the main screen. Channels three through eight are set the same way but the *degrees F* setting is entered. After *degrees F* has been selected, the type of thermocouple is selected (in this testing J-type). The allotted time between recorded data points that the Hydra will store can also be programmed. By pressing the interval button on the front of the Hydra and then using the arrow keys, a specific interval can be set. The interval setting windows are from as low as one second to as high as nine hours (in this testing ten minutes). After selecting the targeted time interval, pressing enter will store the selection and exit the interval option screen. Holding the shift button while pressing the print button gives the option of clearing out any previously stored data, which is a good idea before any test. To ensure that the Hydra is going to store all programmed channels, press the shift button and then the print button. The word Store will appear on the screen. By hitting enter twice, the Hydra will be in a store all mode. The Hydra is now ready to begin collecting data. The last step is pressing the scan button

on the Hydra which tells it to begin collecting data. This step should not be acted out until the test is fully ready to begin. If at any time during testing, a voltage or temperature wants to be observed, there is a monitor button.

The opposite ends of the two leads that are installed in channel one of the Hydra, are used to retrieve a voltage drop across the desired SSRs. One lead is mounted into the terminal block corresponding to the first SSR while the second lead is placed in the last terminal block for the last SSR (Figure 3.2.10). Because there are more than one target powers, locations of these leads will change.

The opposite ends of the two leads discussed above for channel two can now be connected to the VaryAc current banana jacks. This particular channel will record the voltage drop across the shunt resistor. Just above the current banana jacks are the voltage banana jacks. The load voltage leads are connected here with their opposite ends connected to the first SSR (in series) terminal blocks. The last SSR in series will have leads coming out of the corresponding terminal blocks and continuing to the resistive load. The fan is placed approximately two feet from the load banks to create a constant air flow across the resistors.

The power supply is now ready to be programmed. The GW PSP -405 has a voltage set limit. By pressing the V limit button, then the arrow key facing up, the voltage limit is set for 25.01 volts. This ensures the SSR input has enough voltage and current to conduct while the control is turned on. In order to energize the relays, press output on the power supply. There are red and black banana jacks on the front of the GW PSP -405. The two jacks are used to connect the conducting wires that will carry the

energy from the power supply to the RM3 boards. Because each SSR input is connected in parallel using the RM3 boards, they will each turn on simultaneously.

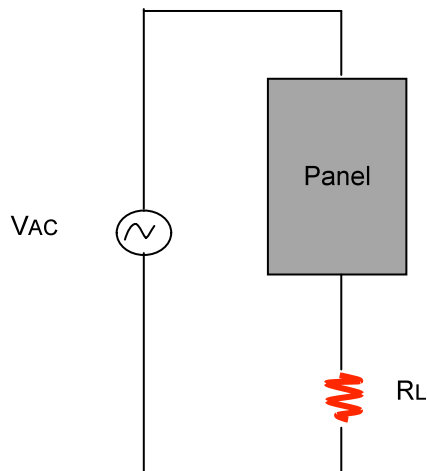


**Figure 3.2.14: Overall schematic of test**

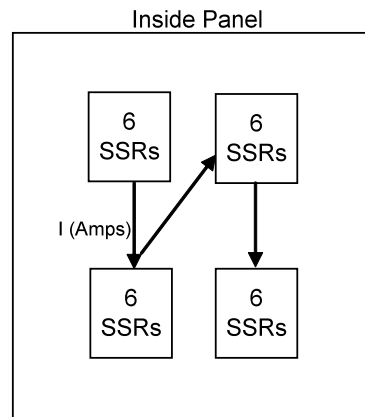


**Figure 3.2.15: Series circuit inside panel**

The two figures above show the general circuitry of the test design. The arrows in Figure 3.2.15 describe the current flow when all four heat sinks are connected in series. Because of the supply current limitation of 18 amps of the variac used in the testing of the relays, it is not possible to test all 24 solid state relays in parallel. Therefore, all 24 solid state relays are connected in series to simulate 24 SSRs being switched on at the same time in the field. This will create maximum heat dissipation inside the panel.

## CHAPTER 4

### TESTING AND DATA ANALYSIS

#### 4.1 Targeted Powers

Testing begins with a targeted power of 100 watts inside the panel along with the recording of heat build up at the five heights. There are 24 SSRs in series with each other. Each heat sink bank has six relays so that there is a combined four banks. This first test requires ten finned heaters in series for a total un-energized load resistance of  $85 \pm 3 \Omega$ . The variac is set to deliver 134.1 volts (AC) when toggled in the “on” position. By pushing the output button on the controller, the scan button on the Hydra, and turning the fan on at middle speed, the test begins. The following table is the Hydra’s recorded data. Starting from left to right is channel one through eight. Subtracting the ambient temperature (Chnl. 8) from the temperature at five foot inside the panel (Chnl. 7) on each row, a maximum change in temperature can be found. This particular row is then used to find all change in temperatures. Table 1 has these five temperatures highlighted in yellow.

Table 4.1.1: Downloaded hydra information

VDrop (In Panel)	VDrop (Across shunt)	Current	Power (In Panel)	"F" 1 Ft.	"F" 2 Ft.	"F" 3 Ft.	"F" 4 Ft.	"F" 5 Ft.	"F" Ambient	"delta "F" 5 Ft.
9.54	0.098	9.76	93.09	71.07	71.32	71.64	71.93	72.47	69.58	2.89
9.33	0.099	9.87	92.09	70.83	71.32	71.77	72.46	74.26	71.03	3.24
9.23	0.099	9.86	91.02	71.17	71.71	72.37	73.49	75.80	71.68	4.12
9.12	0.099	9.85	89.81	71.55	72.20	73.06	74.64	77.52	71.60	5.92
9.06	0.099	9.87	89.42	71.99	72.71	73.82	75.85	79.53	71.90	7.63
9.04	0.099	9.87	89.15	72.50	73.30	74.67	77.01	81.40	73.07	8.34
9.01	0.098	9.85	88.67	73.02	73.79	75.50	78.16	82.66	73.24	9.42
8.96	0.099	9.86	88.35	73.36	74.22	76.16	79.07	83.71	72.42	11.30
8.94	0.098	9.84	87.97	73.66	74.57	76.69	79.88	84.86	73.89	10.98
8.92	0.098	9.82	87.56	73.99	74.99	77.42	80.75	85.81	73.53	12.28
8.94	0.098	9.82	87.81	74.35	75.38	77.98	81.43	86.68	73.25	13.42
8.91	0.098	9.82	87.57	74.63	75.63	78.43	82.02	87.53	73.12	14.42
8.97	0.098	9.80	87.91	74.88	75.91	78.88	82.55	88.04	73.14	14.90
8.97	0.097	9.72	87.19	75.13	76.19	79.30	83.03	88.65	72.50	16.15
8.98	0.098	9.78	87.86	75.19	76.39	79.58	83.37	88.93	73.36	15.57
8.99	0.097	9.72	87.44	75.50	76.70	80.06	83.90	89.49	73.70	15.80
8.89	0.097	9.71	86.36	75.76	77.02	80.44	84.31	89.92	72.76	17.17
8.87	0.098	9.78	86.72	75.85	77.17	80.62	84.54	89.96	73.34	16.62
8.96	0.097	9.70	86.92	75.95	77.37	80.88	84.78	90.42	73.57	16.85
8.94	0.097	9.68	86.50	76.13	77.62	81.18	85.08	90.49	73.24	17.25
8.95	0.097	9.74	87.22	76.18	77.72	81.40	85.26	90.96	72.98	17.98
8.95	0.097	9.73	87.03	76.30	77.93	81.58	85.47	91.40	73.76	17.64
8.93	0.097	9.72	86.84	76.45	78.13	81.83	85.73	91.66	73.30	18.26
8.94	0.096	9.64	86.14	76.57	78.29	81.99	85.91	91.80	73.11	18.69
8.93	0.097	9.73	86.86	76.61	78.38	82.09	86.01	91.48	73.73	17.75
8.92	0.097	9.70	86.51	76.80	78.57	82.30	86.22	91.80	73.79	18.00
8.91	0.097	9.69	86.30	76.93	78.70	82.43	86.38	91.74	73.27	18.46
8.90	0.097	9.69	86.25	76.97	78.80	82.53	86.48	91.92	73.23	18.59
8.77	0.101	10.09	88.46	77.04	79.01	82.71	86.63	92.24	74.16	18.08
8.77	0.100	10.00	87.67	77.23	79.14	82.87	86.87	92.34	73.77	18.57
8.78	0.100	10.05	88.17	77.32	79.29	83.02	87.02	92.48	73.69	18.80
8.77	0.100	10.01	87.85	77.37	79.39	83.15	87.18	92.42	73.59	18.83
8.77	0.100	10.01	87.83	77.42	79.41	83.20	87.23	92.55	73.61	18.94
8.76	0.101	10.07	88.17	77.45	79.56	83.23	87.32	92.58	73.85	18.74
8.76	0.100	10.03	87.85	77.55	79.66	83.42	87.45	92.65	74.00	18.65
8.77	0.100	10.01	87.80	77.63	79.74	83.55	87.61	93.19	73.69	19.50
8.76	0.100	10.01	87.76	77.65	79.84	83.63	87.80	93.29	73.53	19.76
8.76	0.100	10.03	87.86	77.68	79.91	83.69	87.84	93.27	73.31	19.96
8.75	0.101	10.06	88.04	77.66	79.94	83.75	87.89	93.21	72.77	20.45
8.74	0.100	10.02	87.54	77.61	79.98	83.76	87.91	93.23	74.04	19.19
8.74	0.100	10.04	87.79	77.73	80.04	83.85	88.05	93.40	73.47	19.93
8.73	0.100	10.03	87.61	77.77	80.10	83.95	88.12	93.41	73.48	19.93
8.74	0.100	10.03	87.67	77.71	80.05	83.92	88.10	93.50	73.51	19.98
8.74	0.100	10.03	87.67	77.75	80.15	83.93	88.16	93.45	73.98	19.47
8.73	0.100	10.04	87.57	77.81	80.20	84.02	88.19	93.59	73.21	20.38
8.73	0.100	10.02	87.54	77.79	80.22	84.00	88.23	93.60	73.85	19.75
8.75	0.100	10.03	87.74	77.82	80.22	84.06	88.23	93.66	73.85	19.81
8.72	0.101	10.06	87.76	77.90	80.29	84.10	88.36	93.73	73.24	20.50
8.73	0.100	10.02	87.48	77.90	80.32	84.07	88.33	93.68	73.24	20.44
8.70	0.101	10.05	87.43	77.85	80.27	84.06	88.28	93.60	73.70	19.90
8.70	0.100	10.04	87.39	77.96	80.28	84.09	88.32	93.64	73.71	19.93
8.70	0.101	10.06	87.53	77.85	80.33	84.11	88.31	93.77	72.76	21.01
8.69	0.101	10.07	87.52	77.75	80.23	84.04	88.21	93.53	72.97	20.56
8.69	0.101	10.08	87.56	77.75	80.20	84.01	88.27	93.61	73.35	20.27
8.69	0.100	10.04	87.27	77.76	80.27	83.99	88.28	93.60	73.61	19.98
8.70	0.100	10.04	87.32	77.76	80.27	84.08	88.28	93.68	73.38	20.30
8.72	0.100	10.02	87.37	77.79	80.24	84.03	88.28	93.54	73.30	20.24
8.69	0.101	10.06	87.44	77.78	80.29	84.04	88.30	93.62	72.89	20.73
8.68	0.100	10.04	87.16	77.74	80.22	84.01	88.27	93.55	72.97	20.58
8.70	0.100	10.05	87.42	77.65	80.21	83.94	88.23	93.63	72.90	20.73
8.68	0.101	10.07	87.42	77.60	80.16	83.98	88.20	93.55	72.62	20.93
8.69	0.101	10.06	87.43	77.54	80.11	83.89	88.12	93.47	72.68	20.79
8.69	0.101	10.06	87.46	77.54	80.13	83.89	88.15	93.58	73.62	19.95
8.71	0.101	10.05	87.55	77.68	80.11	84.03	88.29	93.75	73.85	19.90
8.69	0.101	10.12	87.92	77.77	80.22	84.04	88.32	93.69	72.48	21.21
8.72	0.101	10.06	87.70	77.72	80.26	84.04	88.32	93.87	73.49	20.38
8.72	0.101	10.07	87.79	77.85	80.30	84.17	88.40	93.83	73.53	20.29
8.70	0.101	10.11	87.94	77.86	80.28	84.12	88.41	93.75	72.74	21.01
8.71	0.101	10.08	87.78	77.81	80.26	84.08	88.42	93.88	73.41	20.47
8.70	0.101	10.09	87.81	77.86	80.31	84.16	88.50	93.81	73.52	20.29
8.72	0.101	10.10	88.11	77.92	80.34	84.24	88.49	93.66	73.09	20.47
8.71	0.101	10.09	87.86	77.83	80.28	84.15	88.46	93.81	73.11	20.70
8.71	0.101	10.10	87.96	77.91	80.39	84.20	88.54	93.92	73.25	20.67
8.70	0.101	10.11	87.91	77.99	80.42	84.31	88.63	93.97	73.39	20.58
8.69	0.101	10.14	88.09	78.06	80.45	84.35	88.69	93.90	73.26	20.64
8.69	0.101	10.13	88.09	77.99	80.42	84.29	88.57	93.83	72.53	21.30
8.70	0.101	10.10	87.87	77.92	80.43	84.24	88.61	93.67	73.01	20.67
8.68	0.101	10.11	87.71	77.98	80.43	84.33	88.64	94.01	73.01	21.01
8.69	0.101	10.13	88.06	78.10	80.52	84.42	88.70	93.93	73.10	20.84
8.67	0.102	10.16	88.02	78.15	80.60	84.50	88.81	93.87	73.18	20.69
8.68	0.101	10.15	88.05	78.16	80.64	84.54	88.82	94.05	72.59	21.47
8.71	0.101	10.09	87.91	78.07	80.58	84.45	88.73	93.93	72.84	21.09
8.72	0.101	10.07	87.80	78.07	80.58	84.44	88.79	94.02	72.95	21.06
8.70	0.101	10.10	87.83	78.13	80.58	84.51	88.82	94.14	72.85	21.29
8.72	0.101	10.10	88.10	78.17	80.63	84.52	88.86	94.01	72.92	21.09
8.71	0.101	10.12	88.20	78.18	80.63	84.53	88.90	94.13	72.78	21.35
8.73	0.101	10.12	88.31	78.08	80.53	84.40	88.74	94.08	72.56	21.52
8.72	0.101	10.14	88.36	78.03	80.54	84.41	88.75	94.09	72.74	21.35
8.71	0.101	10.14	88.31	78.08	80.59	84.49	88.83	94.23	73.11	21.12
8.71	0.101	10.14	88.01	78.08	80.62	84.51	88.88	94.14	72.52	21.52
8.70	0.101	10.14	88.18	78.02	80.56	84.43	88.77	94.25	72.73	21.52
8.69	0.101	10.13	88.00	78.05	80.59	84.49	88.83	94.23	72.94	21.29
8.71	0.101	10.14	88.29	78.11	80.59	84.52	88.92	94.26	72.91	21.35
8.70	0.101	10.14	88.24	78.09	80.57	84.49	88.83	94.01	72.40	21.61
8.69	0.101	10.14	88.11	77.97	80.56	84.43	88.80	94.23	72.88	21.35
8.70	0.101	10.08	87.67	78.03	80.60	84.49	88.89	94.18	73.11	21.06
8.75	0.101	10.06	86.90	78.03	80.54	84.52	88.86	94.18	72.00	21.18
8.75	0.100	10.05	87.95	77.96	80.50	84.37	88.74	94.14	72.96	21.18
8.75	0.101	10.06	88.06	77.92	80.51	84.41	88.84	94.09	73.03	21.06
8.76	0.100	10.04	87.97	78.00	80.57	84.46	88.83	94.15	73.06	21.09

The power dissipation corresponding to the above data is the average voltage drop over the relays (Chnl. 1) multiplied by the load current (Equation 2).

$$P_{Dissipated} = I_{Load} * V_{Drop(SSR)} \quad (2)$$

The current used in Equation 2 is the voltage drop over the shunt resistor (Chnl. 2) divided by the known shunt resistance (0.01  $\Omega$ ).

$$I_{Load} = \frac{V_{Drop(Shunt)}}{R_{Shunt}} \quad (3)$$

Equation 3 utilizes Ohms law ( $V=IR$ ). Each test is conducted until equilibrium temperature conditions are reached (Figure 4.1.1).

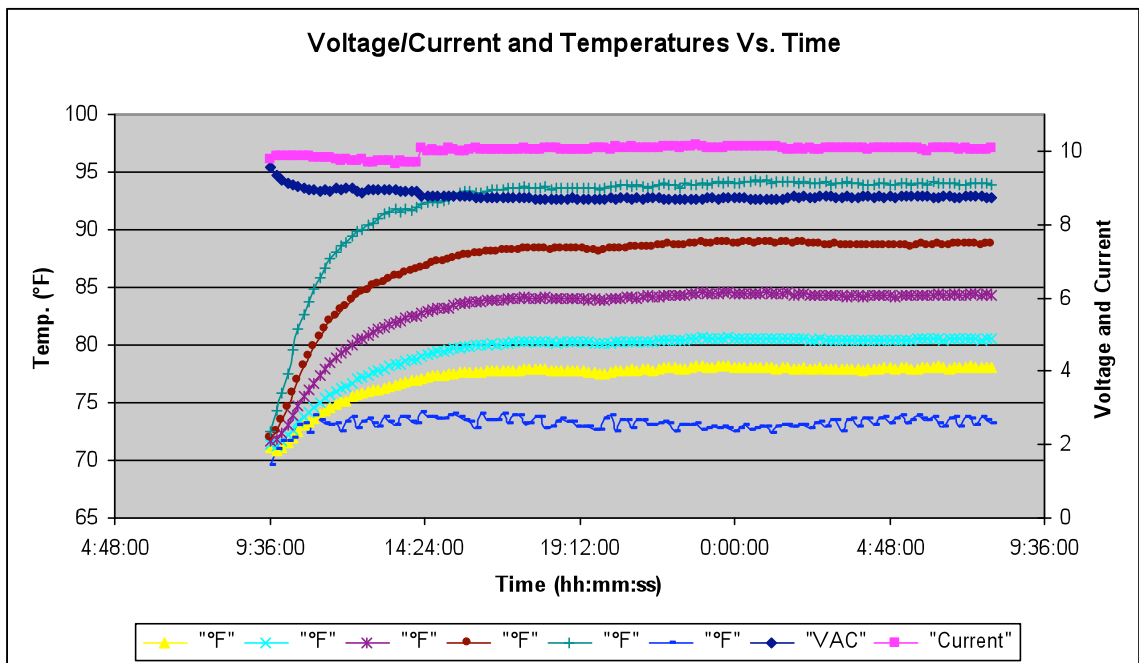


**Figure 4.1.1: Equilibrium conditions**

The same procedure is continued in order to receive enough data points to plot the change in temperature (delta T) versus power. Different powers are established by changing the size of the load resistance as well as changing the voltage. A plot is configured containing numerous powers and their corresponding change in temperatures at one, two, three, four, and five feet inside the panel. The following graph shows the change in temperature versus power at these corresponding heights.

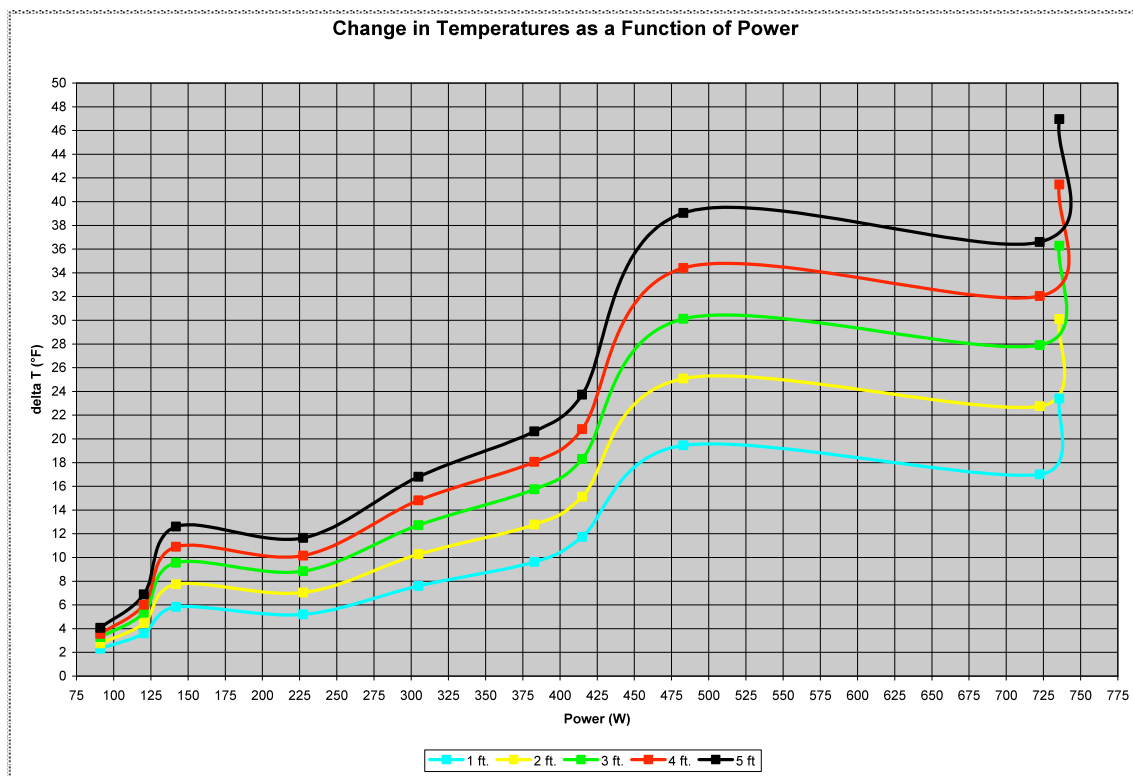


**Figure 4.1.2: Change in temperature versus power**

As seen in the graph in Figure 4.1.2, there is a non-linear response to the temperature versus power curve. The beginning assumption that a linear power to heat relationship will occur when energizing SSRs in series does not seem to be valid. The test must be reexamined and altered in order to achieve the original goal. At this junction, analysis becomes easier by focusing on just one height in the panel. The graph above shows that each height contains the same slope so by analyzing just one height, the same can be said for the other four heights. The five foot mark inside the panel is chosen. This is an arbitrary choice for the following examinations, but since this point is the hottest in the panel, the end result may cause for this to be the deciding factor on whether or not maximum heating has taken place inside the panel. Focusing on the five foot plots,

there is an obvious linearity between specific powers despite the overall non-linearity (Figure 4.1.3).

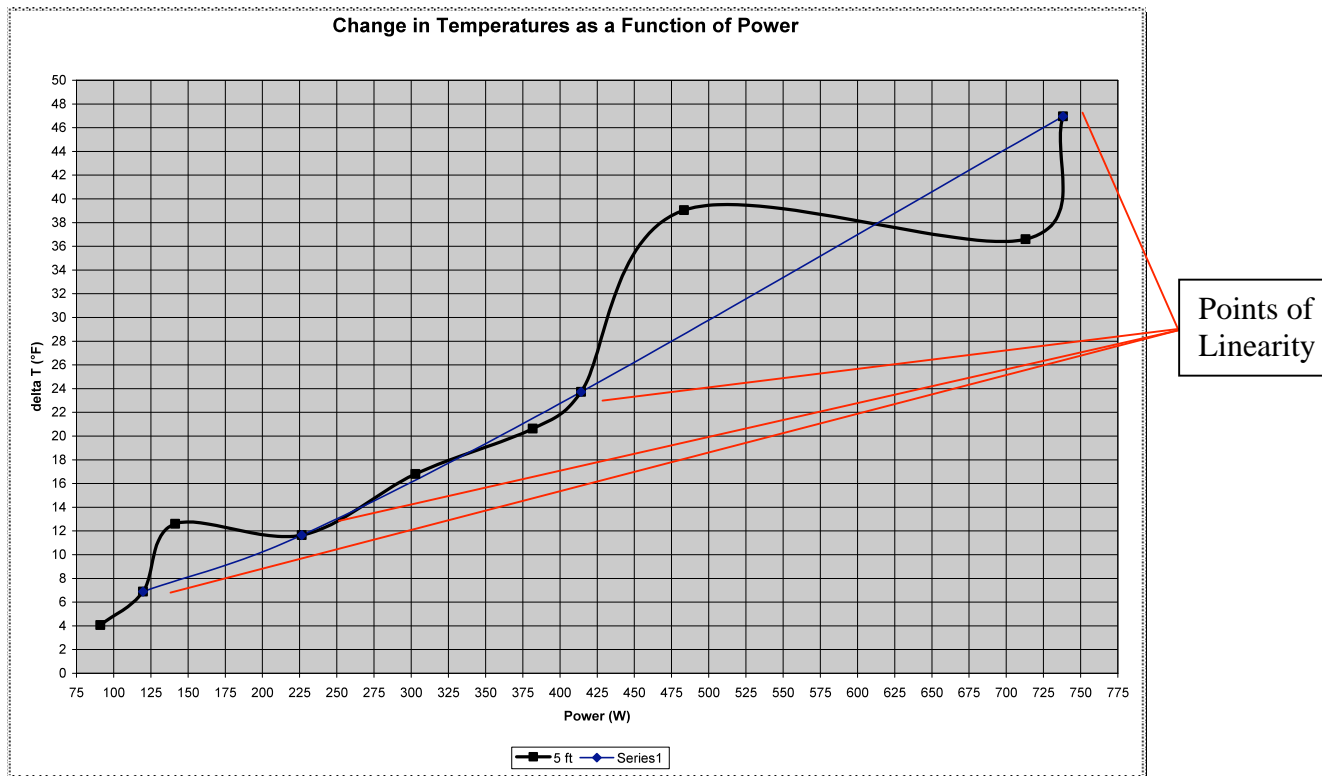


**Figure 4.1.3: Change in temperature versus power with linear similarities**

Questions concerning the results thus far must first be evaluated before continuing with experimentation. What do these four points have in common? Why does the SSR allow the above data to occur? How can the test be reconfigured so that there may be a final, linear change in temperature as a function of power?

In order to answer the first question, locate the four linear points from the downloaded data. Once, these data are collected, a clear common voltage AC is applied to these four points (Table 4.1.2).

**Table 4.1.2: Similar voltages from graph**

Power (watts)	Voltage (ac)
119.75	148.80
226.47	148.80
414.14	146.00
738.14	147.00

At this juncture in the test, the decision is made that keeping a relatively constant voltage AC leads to a more linear fit. If the voltage cannot be altered greatly then the resistive load must be altered in order to vary current. Already there is another problem. In trying to run the first test, which has a goal of one hundred watts through the panel, a high enough current cannot be obtained because of resistive load limitations. This of course is a large problem, because the following testing requires higher currents in order to reach 250, 500, and 750 watts. Further analysis reveals the following. The voltage drop across six SSRs in series with 140 volts (AC) is 9.31 V. Using Equation 1 along with the desired 100 watts and 9.31 V, then solving for current, yields a 0.86 amperes current. Next, using Equation 2 and substituting Ohms law for voltage, a load resistance of 0.87 ohms is equated.

$$P = I^2 R \quad (4)$$

There is a total of ten finned resistors. With all ten resistors in parallel equation three is used to find that the total resistance is equal to  $0.85 \pm 0.3 \Omega$ .

$$\frac{1}{R_T} = \frac{1}{R_1} + \frac{1}{R_2} + \dots + \frac{1}{R_{10}} \quad (5)$$

Initially this is a good resistance to have. Unfortunately these are finned resistors and as they heat their resistance will climb which will in turn decrease the current through the panel. The power then decreases and 100 watts can not be achieved. The bigger problem with this method of testing is that the resistance must decrease much more in order to

receive an even higher current for the 250, 500, and 750 watt targets. Once again the test procedure must be reevaluated. The voltage must be kept as constant as possible and the load must remain the same. The only other variable to change is the voltage drop across the relays. This can be achieved by adding more relays in order to increase the voltage drop and therefore increase the power that travels through the panel.

Before the testing continues, now is a good time to answer the second of the questions. What characteristic of the SSR allowed the nonlinear data to occur? A simple test is created in order to examine the uniqueness of one relay and then apply these physical parameters to the above data. The load resistance used in this test will be the same finned resistor as before except there are ten total in series. This test involves just one HD6050 relay in series with the load. A 120 voltage AC variac will be used to apply the output voltage as well as the same power supply for the input control. The Wavetek 320 B is used to manually record amperage while the same Fluke 87 III True RMS Multimeter is used to manually record the AC voltage as well as the voltage drop across the relay. The AC voltage is ramped from five volts to 120 volts in five volt intervals. The AC voltage is continued from 120 volts to 190 volts (variac maximum) but in ten volt intervals. At each interval, voltage AC, load amperage, and voltage drop across the solid state relay are recorded in an excel spreadsheet. Equation 2 and 3 are applied to the data in order to find the power through the SSR as well as the resistance for each interval. Next, use this information in combination with Excel's graphing features to plot the SSR performance with regards to the previously found data (Figure 4.1.4).

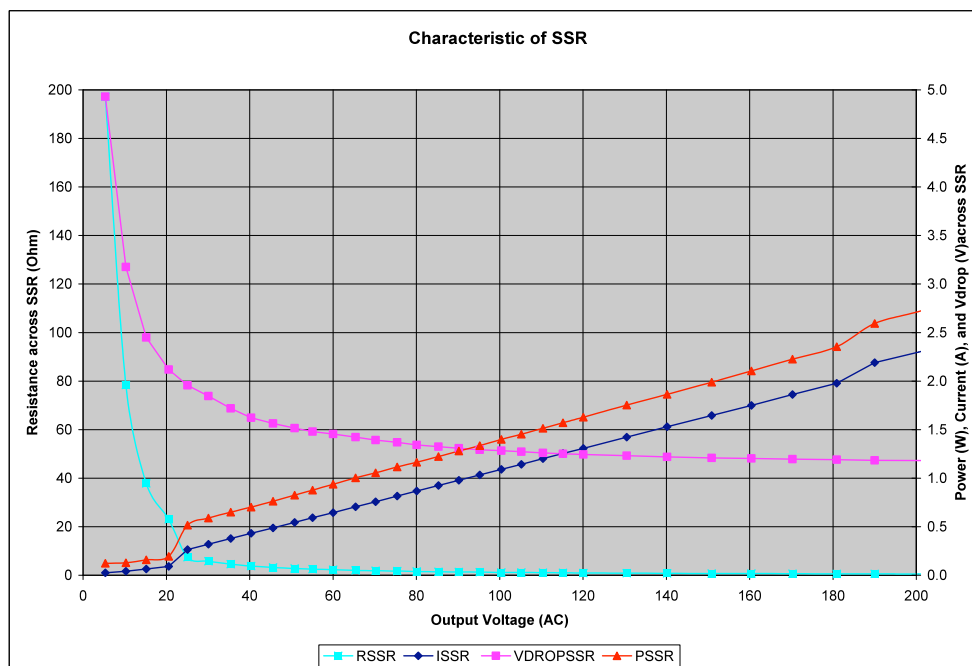


**Figure 4.1.4: Characteristic of SSR**

Notice the power, current and voltage drop across the solid state relay are on a secondary axis. The figure above shows the relay's resistance decays exponentially as the output AC voltage is increased. As a result, the voltage drop across the relay is exponentially decreasing as well. This non-linear region occurs because the triac that is formed from the parallel SCRs behaves nonlinearly. There has to be a minimum gate voltage for each SCR to reach an initial "on" state. Once in the "on" state, the additional biasing of the triac creates an exponential increase in current and decreases the voltage drop due to the diode response. Around 50 volts AC the SSR begins to settle into its nominal voltage drop range but does not reach full conductance until 120 volts AC. There is an obvious inverse relationship between the power and voltage drop of the solid state relay until in the nominal operating range (Figure 4.1.4). Once in the manufactured operating range the voltage drop will no longer continue to vary while power through the relay is increased. By simply making sure there is enough output AC voltage applied to each

SSR in order to reach their full conductance range (minimal voltage drop), the test should yield linear results. Since this range is around 120 volts with a less than or equal to 1.25 volts dropped across each relay, there must be at least 127.5 volts applied to one of the heat sink banks that contains 6 SSRs. If another bank was added in series, 135 volts would have to be applied. If a third bank was added, 142.5 volts AC would have to be applied and a fourth bank would require 150 volts AC. The problem with testing in this manner, are the limitations in the test equipment. With the total voltage drop across 24 SSRs at 30 volts, in order to achieve a power of 750 watts, there would have to be a current of 25 amperes. For a second targeted power of 500 watts and the same nominal voltage drop across the relays, the test would require 16.67 amperes. The limitations on the amperage through the variac have now become a problem. These problems are solved in order to acquire the necessary data by adding an additional voltage source. Now the necessary power through the panel can be achieved with two different circuits containing 12 SSRs in series.

With the necessary solutions to the problems analyzed and resolved testing can continue. The goal of the following testing is the same as the original. There needs to be a minimum of three data points in order to have desired results. These three data points will consist of three different powers inside the panel along with their corresponding temperatures inside the panel. Once these powers are achieved alterations will be made to the panel's internal air circulation (installing fans and vents) in order to cover all scenarios for a heat tracing panel. Both the procedure and method of data analysis will remain the same as the previous testing. The voltage applied to the output side of the relay will remain considerably more constant for all three tests. The voltage will have to be

increased slightly as re-lays are added to the series circuit. This voltage is increased only enough to receive a desired minimum voltage drop across the relays. Initial testing will be with the panel in original form. The first of these three powers is one hundred watts. One hundred watts can be obtained using one SSR bank (6 relays). The voltage AC is held constant at  $140 \pm 0.3$  volts. The load resistance consists of just one of the finned heaters which equaled an initial non-energized resistance of  $8.5 \pm 0.1$  ohms. The previous two measurements are taken using a Fluke 87 III True RMS Multimeter. The next targeted power is 250 watts. Adding another SSR bank in series with the original will increase the total voltage drop through the panel which in turn increases the power. The voltage (AC) is increased to  $160 \pm 0.3$  volts in order to obtain maximum conduction per relay. In other words, since each relay requires a minimum amount of voltage to conduct properly and these relays are in series, then there is a voltage drop across each re-lay leaving less total voltage for the following relay. If initial voltage is not increased then the final relays will not receive the proper conducting voltage. The third test is slightly more complex than the initial two. Because of all the restrictions that have risen due testing as well as equipment, a second variac must be used. By bringing in a second voltage source, two circuits containing the same design as the 250 watt test will result in a total 500 watt test. The first circuit is two load banks in series on the left side of the panel. The second circuit is two load banks in series on the right side of the panel (refer back to Figure 3.2.15). Each circuit will contain one finned resistor in series for the load resistance. One problem with this setup is once again the limitations in the equipment. There is only one variac containing a shunt resistor with a small enough resistance. The other shunt resistors contain a higher resistance ( $1.0 \Omega$ ), which will cause too great a

power across it. The power across the shunt (Equation 6) is found by substituting Equation 2 into Equation 1 for the voltage drop across the shunt.

$$P_{Shunt} = I_{Load}^2 R_{Shunt} \quad (6)$$

Using these equations along with the shunt resistance and a load current of roughly 12 amperes, the power across a 1.0 ohm resistor would be 144 watts. These particular shunt resistors are rated at a maximum of 25 watts. This is the reason for the installation of the 0.01 ohm shunt resistor previously discussed. An overload in power across the shunt will cause the shunt to burn up. In order to record the data on both circuits, two tests are run. The first test will consist of data being recorded on one side of the panel and the second will be the same test conducted again but this time data on the other side of the panel will be recorded. Keep in mind that during the two tests, both circuits have power. Once both tests are completed the power through the circuit of one test is added to the power of the other. Now that four tests are complete and three powers have been obtained, plot the change in temperature versus the power. The following graph shows the plots at the five different heights inside the panel.

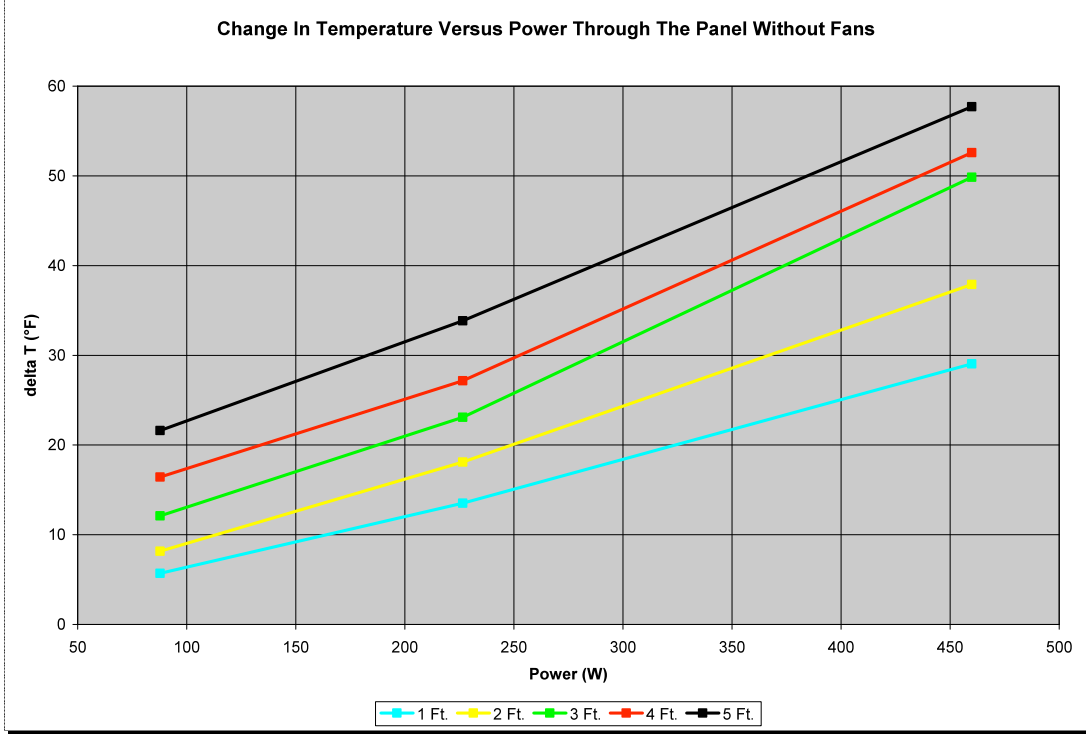


**Figure 4.1.5: Change in temperature versus power (two)**

The graph also provides the necessary linearity that is targeted for this experimentation. All the three questions have now been answered. The testing can be completed with the installation of fans and vents so that outside air can be used to cool the environment inside the panel.

4.2 Installation of Fans and Vents

The testing in section 4.1 concluded with the data found in Figure 4.1.5. The same testing is conducted again but with four more different scenarios. These different scenarios are achieved by cutting holes in the panel so that cooling fans (TFP41UL12) and exhaust grilles (TEP4UL12) can be installed. Using a plasma cutter, a total of four holes are cut. There are two cut in the top of the panel for the exhaust grilles (vents).

These holes are placed in the center of the top of the panel with a distance of approximately 6 ¼ inches separating them (Figure 4.2.1).

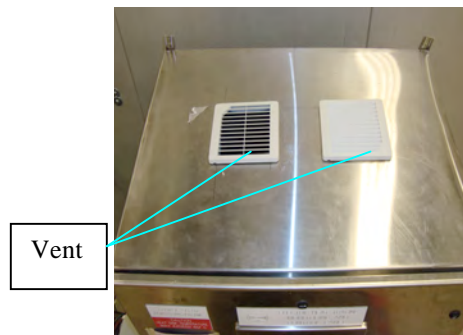


**Figure 4.2.1: Top view of panel**

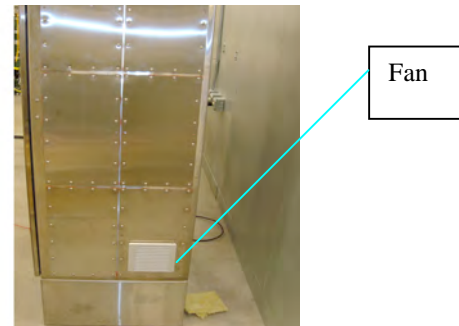


**Figure 4.2.2: Right exterior view of panel**

The plasma cutter is now used to cut two holes for the fans in the side cover plates that are mounted to the panel. The fans are located at the bottom of the panel, furthest from the vents to ensure maximum distance between the fans and vents (Figure 4.2.2). One fan is placed on the right side of the panel while another is placed on the left side of the panel. The maximum distance will produce maximum air flow throughout the panel.

Now that the installation of the fans and vents is complete the testing continues. The first of the different scenarios is both fans being on and both vents open. The next scenario consists of a simulated one fan broken test. This is achieved by simply turning one of the fans off. After this situation is tested, insulate the fan that is shut off. Now a one fan and two vents situation can be analyzed. The last test is with one fan and one vent. This scenario is produced by insulating the vent that is on the same side of the panel as the operating fan. This once again creates maximum distance between entering and exiting air for maximum air flow.

### 4.3 Results

All data can now be comprised and plotted (Figure 4.3.1) showing the change in temperature versus power.

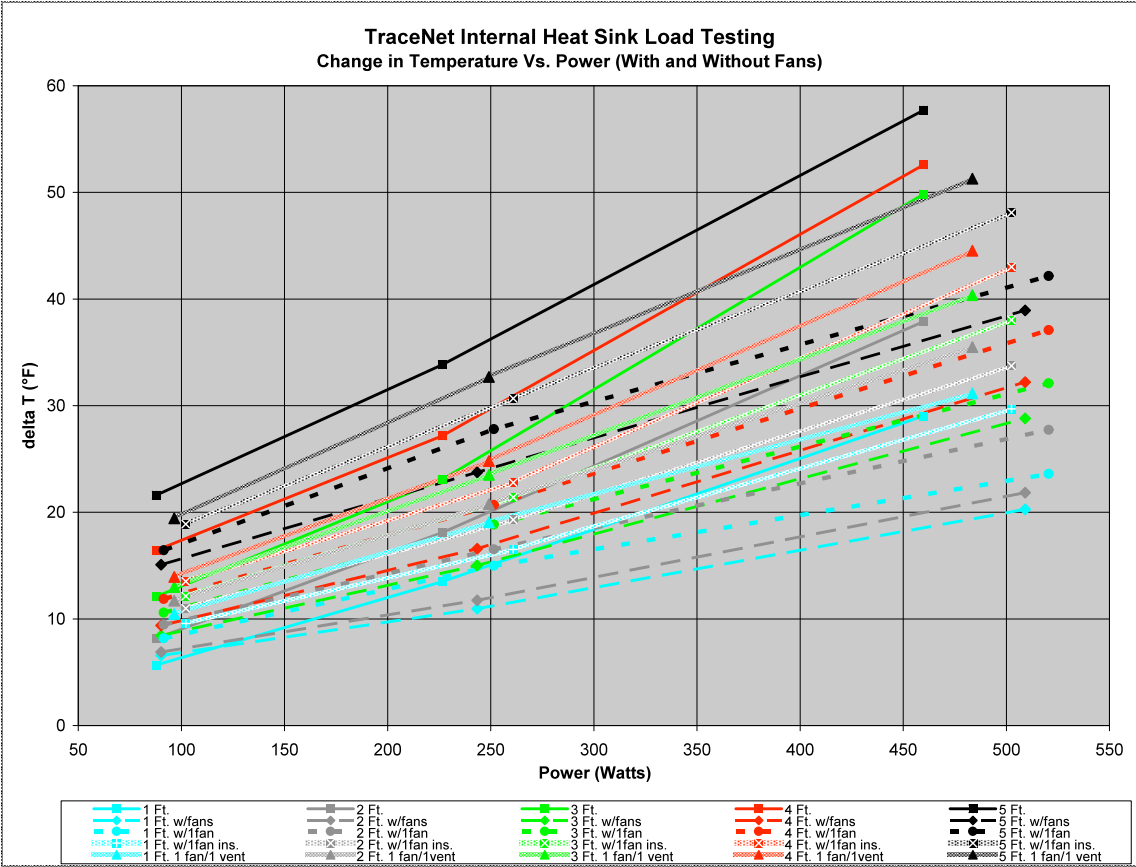
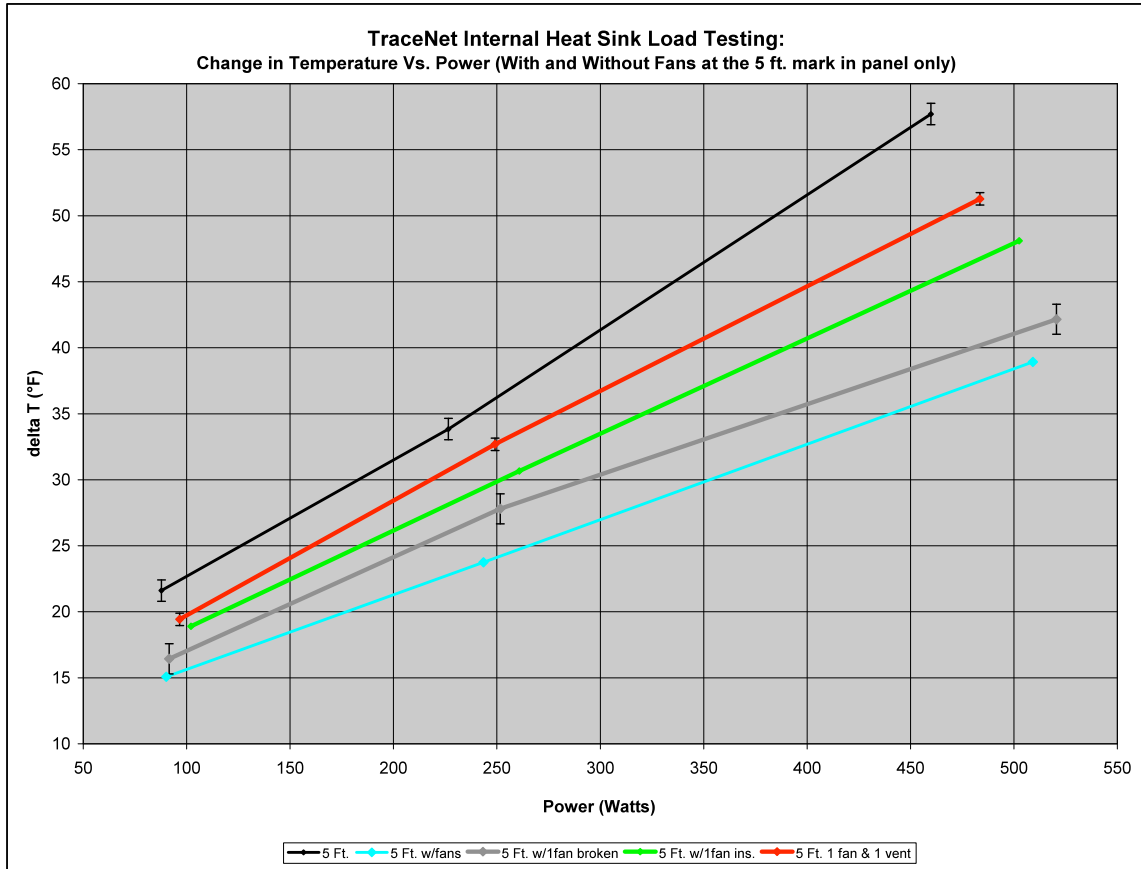


Figure 4.3.1: Change in temperature versus power (three)

Due to the visual complexity of the graph, a simpler one is formed with only the data taken at the five foot mark thermocouple inside the panel (Figure 4.3.2). This particular location is chosen to further analyze because this is the hottest point in the panel.



**Figure 4.3.2: Change in temperature versus power at five feet inside panel**

Using Excel's best fit trend line, an equation for each of the above lines can be found. The trend line equations can then be used to plot a final change in temperature versus power from 100 to 750 watts. This plot appears below with error bars included when using no fans, one fan / one vent, and one fan broken situations.

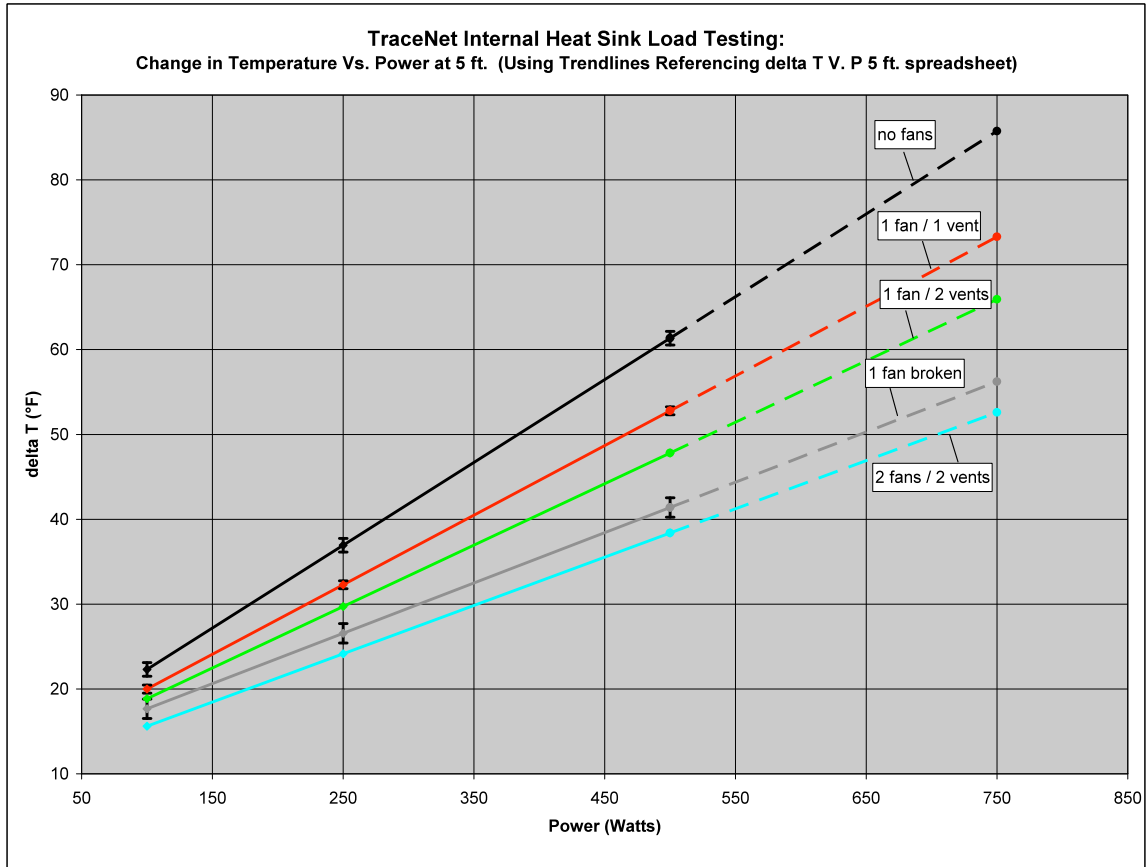


**Figure 4.3.3: Overall performance at five feet inside panel**

The amount of error is found by comparing the best fit line to the experimental one.

Taking the difference between the two will give the length of the error bars. The overall performance of the power increase inside the panel stayed well under the manufactured maximum temperature of the relay of 125 °C (250 °F).

## **CHAPTER 5**

### **DISCUSSION**

The original testing produced non-linear data. After analyzing the performance of just one solid state relay, proper conductance is found in the linear regime. Proper conductance is necessary because only at this condition will the SSR produce the most heat. The result of the single SSR test shows the inverse relationship between voltage drop and power until the SSR is within the optimal operating range. This operating range is stated in the Crydom solid state relay manual, but without explicit explanation. Numerous discussions with Thermon employees as well as the vice president of Crydom (Brian Bixby), led to the realization that these particular relays are difficult to test when aligned in series. Due to the solid state triac switching device, each relay needs a relatively large voltage across the output terminals. The required voltage will conduct the relay into a linear range instead of the initial non-linear results. The original design of the solid state relay is for each relay to operate as an independent switch. The 750 watt temperature versus power data are calculated using empirical data. The end temperature results did remain under the maximum temperature range of the SSRs before breakdown will occur.

## CHAPTER 6

### CONCLUSION

Solid state relays have proven to be very advantageous in the heat tracing industry. There are numerous aspects SSRs contain which allow them to be the switch of choice over the electromagnetic relay. The physical aspects of the SSR are simple at the macro level but complex when looking to the internal design and how they utilize solid state physics. At the macro level the SSR separates output from input with light. The light comes on the SSR switches to the on position. At the micro level the SSR is made up of numerous solid state devices which communicate with each other. The devices signal each other when to turn on and when to turn off with the use of doped semiconductors. Once the relay is turned on, the electronic process of voltage drops, current carrying, and resistive properties result in a tremendous heat loss.

An overall performance of temperature versus power in a specified situation is shown in Figure 4.3.3. Only three out four targeted powers could be produced. The 750 watt power range was out of the experimental capabilities by both the equipment and the design of the solid state relay. The testing underwent alterations in order to fit the original scope. Originally the tests revealed nonlinear results due the solid state devices and exponential aspects in the solid state relay. A separate performance test is analyzed in order to better understand the single SSR. This test reveals a clear linear regime at proper voltages of the relay, which will provide the necessary results. Testing is then

continued and linear results are obtained. In addition, the three targeted temperature versus power data enabled and accurate prediction of the fourth. The data are collected and the results focus on just the highest and hottest point of the panel. Using these results, an over all performance can be predicted for the change in temperature as a function of time. The highest and hottest point is chosen because decisions are made based on worse case situations. The highest temperature in the panel with 750 watts of power is still under the maximum solid state relay temperature (before breakdown). Engineers as well as customers now have the necessary data involved in the decision making process. Each heat tracing system as well as control panel is customized differently in order to fulfill a particular environments needs. The above testing examines some of these situations. These results are now applicable for the future production of panels containing internally installed heat sinks.

## REFERENCES

1. A. Bishop, *Crydom Company Solid-State Relay Handbook* (1986).
2. *Crydom Solid State Relay Specification and Reference Directory* (1998).
3. T. L. Floyd, *Electronic Devices: Conventional Current Version, 7<sup>th</sup> Edition* (Pearson Education, New Jersey, 2005).
4. Schuler, C. A., *Electronics: Principles and Applications* (McGraw-Hill, Boston, 1979).
5. B. G. Streetman and S. Banerje, *Solid State Electronic Devices, 5<sup>th</sup> Edition* (Prentice Hall, New Jersey, 2000).

## VITA

Nicholas Alan Miller was born in New Braunfels, Texas, on January 21, 1981. He is the middle child and only son of Joyce Hughson and Kenneth Miller. He is a graduate from New Braunfels High School in 1999 and in the following year attended Incarnate Word University. After only a year at Incarnate Word, he transferred to, what was known as Southwest Texas University in San Marcos. Shortly after Southwest Texas University changed their name to Texas State University-San Marcos, he graduated with a degree of Bachelor of Science in May of 2007. In the following fall semester he began his graduate school at Texas State. A year after his enrollment in the Graduate College of Texas State University-San Marcos, he began working at Thermon. Nicholas is a technical specialist for Thermon and plans on continuing his work at Thermon after graduate school.

Permanent Address: 1218 Oak Ridge Ln.

Canyon Lake, Texas 78133

This thesis was typed by Nicholas A. Miller.